Contrib Mineral Petrol (1990) 105:123–142

Contributions to Mineralogy and Petrology

Corrensite and mixed-layer chlorite/corrensite in metabasalt from northern Taiwan: TEM/AEM, EMPA, XRD, and optical studies

Yen-Hong Shau, Donald R. Peacor, and Eric J. Essene

Department of Geological Sciences, The University of Michigan, Ann Arbor, MI 48109, USA

Received June 19, 1989 / Accepted December 22, 1989

Abstract. Many chloritic minerals in low-grade metamorphic or hydrothermally altered mafic rocks exhibit abnormal optical properties, expand slightly upon glycolation ("expandable chlorite") and/or have excess Al^{VI} relative to Al^{IV}, as well as significant Ca, K and Na contents. Chloritic minerals with these properties fill vesicles and interstitial void space in low-grade metabasalt from northern Taiwan and have been studied with a combination of TEM/AEM, EMPA, XRD, and optical microscopy. The chloritic minerals include corrensite, which is an ordered 1:1 mixed-layer chlorite/smectite, and "expandable chlorite", which is shown to be a mixed-layer chlorite/corrensite. Corrensite and some mixed-layer chlorite/corrensite occur as rims of vesicles and other cavities, while later-formed mixed-layer chlorite/corrensite occupies the vesicle cores. The TEM observations show that the mixed-layer chlorite/corrensite has ca. 20%, and the corrensite has ca. 50% expandable smectite-like layers, consistent with XRD observations and with their abnormal optical properties. The AEM analyses show that high Si and Ca contents, high Al^{VI}/Al^{IV} and low $Fe^{VI}/(Fe+Mg)^{VI}$ ratios of "chlorites" are correlated with interstratification of corrensite (or smectite-like) layers in chlorite. The AEM analyses obtained from 200–500 Å thick packets of nearly pure corrensite or chlorite layers always show that corrensite has low Al^{IV}/Si^{IV} and low $Fe^{VI}/(Fe+Mg)^{VI}$, while chlorite has high Al^{IV}/Si^{IV} and high $Fe^{VI}/(Fe+Mg)^{VI}$. This implies that the trioctahedral smectite-like component of corrensite has significantly lower Al^{IV}/Si^{IV} and $Fe^{VI}/(Fe+Mg)^{VI}$. The ratios of $Fe^{VI}/(Fe+Mg)^{VI}$ and Al^{IV}/Si^{IV} thus decrease in the order chlorite, corrensite, smectite. The proportions of corrensite (or smectite-like) layers relative to chlorite layers in low-grade rocks are inferred to be controlled principally by Fe/Mg ratio in the fluid or the bulk rock and by temperature. Compositional variations of "chlorites" in low-grade rocks, which appear to correlate with temperature or metamorphic grade, more likely reflect variable proportions of mixed-layered components. The assemblages of trioctahedral phyllosilicates tend to occur as intergrown discrete phases, such as chlorite-corrensite, corrensite-smectite, or chlorite-corrensite-smectite. A model for the corrensite crystal structure suggests that corrensite should be treated as a unique phase rather than as a 1:1 ordered mixed-layer chlorite/smectite.

Offprint requests to: Yen-Hong Shau

Introduction

Chlorite is a major secondary mineral in low-grade metamorphic or hydrothermally altered mafic rocks, usually occurring as veins, vesicle-filling materials, and replacements of glassy matrix or olivine crystals. However, many chemical analyses of chlorite from low-grade mafic rocks show deviations from the ideal chlorite formula, especially in a large excess of octahedrally coordinated Al (Al^{VI}) relative to tetrahedrally coordinated Al (Al^{IV}), and significant Ca, Na, and K contents (e.g., Laird 1988). The excess of Al^{VI} over Al^{IV} gives rise to a charge imbalance when formulae are normalized to 10 or 20 cations; it yields large apparent vacancies in octahedral sites when alternatively normalized on the basis of 14 or 28 oxygen atoms. These chloritic materials also exhibit anomalous optical properties when compared with chlorite having normal structural formulae (Albee 1962). Some of these chloritic materials showing expansion with glycolation have been referred to as "swelling chlorite" or "expandable chlorite" (e.g., Kristmannsdóttir 1975; April 1981), while others occur in association with, and have chemical affinities with, corrensite.

As these chloritic materials are the major secondary minerals of alteration or low-grade metamorphism of mafic rocks, the mineral assemblages and their compositions are important clues to understanding the conditions and processes of alteration, metamorphism, or diagenesis. This study has therefore been carried out in order to obtain direct characterization of the detailed chemistry, structure, textures and stacking sequences of

typical low-grade chloritic minerals. These results permit direct interpretation of the complex XRD data that were obtained for the same samples.

Although chloritic minerals having abnormal compositions or optical properties are very common in low-grade rocks, their properties are not well defined. This is in part due to their fine grain size and to their occurrence as heterogeneous mixtures of more than one kind of layer as shown by XRD. The XRD results may be ambiguous, because they are averaged for heterogeneous materials and because inferences regarding stacking sequences may be ambiguous. However, stacking sequences in such materials can be directly resolved using transmission electron microscopy (TEM) and analytical electron microscopy (AEM). For example, TEM and AEM studies have been used to study mixed-layering of chlorite with other phyllosilicates such as talc (Schreyer et al. 1982), biotite (Iijima and Zhu 1982; Veblen and Ferry 1983; Olives et al. 1983; Olives and Amouric 1984; Olives 1985; Eggleton and Banfield 1985), phlogopite (Yau et al. 1984), wonesite (Veblen 1983), illite (Lee et al. 1984; Ahn et al. 1988), and berthierine (Ahn and Peacor 1985). Klimentidis and Mackinnon (1986) and Vali and Koster (1986) have obtained lattice fringe images of well-ordered 1:1 mixed-layer chlorite/smectite with TEM. More recently, TEM and AEM have been used to study mixed-layer chlorite/smectite and corrensite in low-grade metamorphic or hydrothermally altered mafic rocks (Shau et al. 1988; Shau and Peacor 1988; Bettison-Varga and Mackinnon 1989; Shau and Peacor 1989).

Chloritic minerals in a zeolite to prehnite-pumpellyite facies metabasalt from northern Taiwan, like many "chlorites" in low-grade mafic rocks, have a large range of excess Al^{VI} over Al^{IV}, significant Ca content and negative rather than positive optic signs as predicted from their Fe/(Fe+Mg) ratios (Shau and Yang 1987). The variability of their properties and their significance as common rock-forming minerals cause them to be ideal examples of the anomalous chloritic minerals in low-grade rocks. In order to positively characterize these chloritic phases and their stacking sequences, they have been studied by optical microscopy, XRD, electron microprobe analyses (EMPA), and TEM/AEM. Chemical analyses obtained with AEM from packets of well characterized single phases as thin as a few hundred Angstroms permit definition of the differences in compositions of intimately interstratified or intergrown phyllosilicates for the first time. This study was also conducted in order to interpret the anomalies in compositions, XRD, and optical properties of "chlorites" from low-grade rocks, and to understand chemical variations of "chlorite" or assemblages of chloritic materials with respect to metamorphic grades and bulk rock or fluid compositions.

Corrensite was originally defined by Lippmann (1954) as a 1:1 regularly interstratified (or mixed-layered) trioctahedral chlorite/swelling chlorite, and then by Lippmann (1956) as a regular interstratification of chlorite and vermiculite. It has been defined by the Nomenclature Committee of The Clay Minerals Society as a regular 1:1 interstratification of trioctahedral chlorite with either trioctahedral smectite or trioctahedral vermiculite (Bailey 1981). The geological occurrences of corrensite are widespread (Reynolds 1988 and references cited therein). Corrensite has been commonly found in carbonate and evaporite sequences (e.g., Bradley and Weaver 1956; Kopp and Fallis 1974), soils (Johnson 1964), clastic (Earley et al. 1956; April 1981) and volcanoclastic (Almon et al. 1976; Inoue et al. 1984; Chang et al. 1986) sedimentary sequences, and hydrothermal deposits (Shirozu et al. 1975). It also forms by hydrothermal alteration of basaltic or ophiolitic rocks (Alietti 1958; Furbish 1975; Evarts and Schiffman 1983; Brigatti and Poppi 1984a; Alt et al. 1985; Bettison and Schiffman 1988) and weathering of basic igneous rocks (Smith 1960).

The term mixed-layer chlorite/smectite and chlorite/vermiculite have commonly been used to describe trioctahedral sheet silicates that were generally chracterized as interstratified by XRD "bulk-clay" measurements (cf. Reynolds 1988). The term mixed-layer chlorite/corrensite is used in the present study to describe mixed-layered chloritic materials that consist of layers of chlorite and corrensite instead of layers of chlorite and smectite. The terminology for mixed-layered phyllosilicates of Reynolds (1980, 1988) is adopted here. For example, a mixed-layer chlorite(0.75)/corrensite is composed of 75% chlorite layers and 25% corrensite layers. For a completely random ($R=0$) mixed-layer chlorite(0.75)/corrensite, an alternative expression for this stacking sequence is "$R=1$ mixed-layer chlorite(0.8)/smectite" in which the term $R=1$ means that all "smectite" layers are separated by *one* or more chlorite layers if the proportion of chlorite layers $>50\%$. However, those two terms are, strictly speaking, not identical in terms of the crystal-chemical properties of corrensite and smectite. The term mixed-layer chlorite/corrensite used here emphasizes corrensite as a unique phase that constitutes one of the two mixed-layered components.

Experimental methods

Ordinary polished thin sections were prepared for petrographic studies and microprobe analyses, and "sticky-wax"-mounted thin sections for TEM specimens. Following optical study, areas of the thin sections were thinned to approximately 10 μm with a Gatan 656 dimple grinder. Aluminum washers of 3 mm diameter were then attached to these areas with epoxy resin, and the corresponding areas of the sections removed upon gentle heating. They were further thinned using a Gatan 600 ion mill.

The TEM/AEM analyses were obtained using Philips CM-12 and JEOL JEM-2000FX scanning transmission electron microscopes (STEM). The TEM analyses included selected area electron diffraction (SAED) patterns and 00*l* lattice fringe images which were obtained using underfocus (1000–3000 Å) conditions. The AEM-EDS (energy-dispersive spectrometer) analyses were conducted with the Philips CM-12 STEM equipped with a low-angle Kevex QUANTUM detector. The sample was tilted toward the detector by 20°, giving an X-ray take-off angle of 34°. Quantitative analyses were obtained only from thin edges and interpreted using the thin foil approximation (Cliff and Lorimer 1975; Champness et al. 1981). Experimentally determined k values (Cliff-Lorimer factors) were obtained using albite (for Na, Al), clinochlore (Mg, Al,

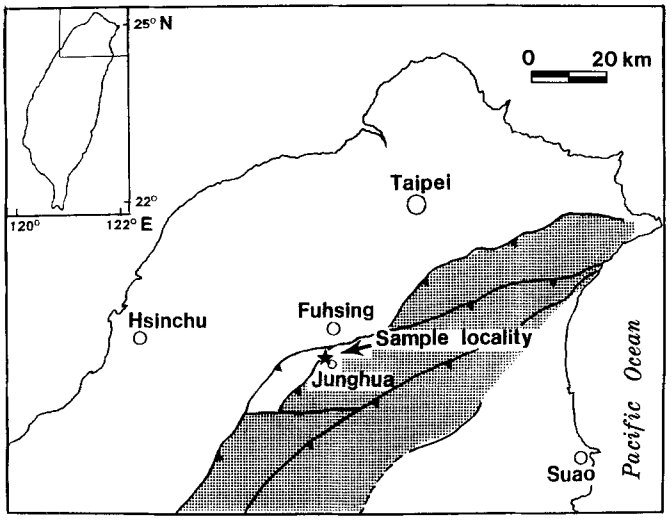

Fig. 1. Locality for samples of Junghua metabasalt in northern Taiwan. The *shaded area* is the Hsuehshan Range, which consists primarily of argillite, indurated sandstone and slate with intercalated meta-basaltic rocks

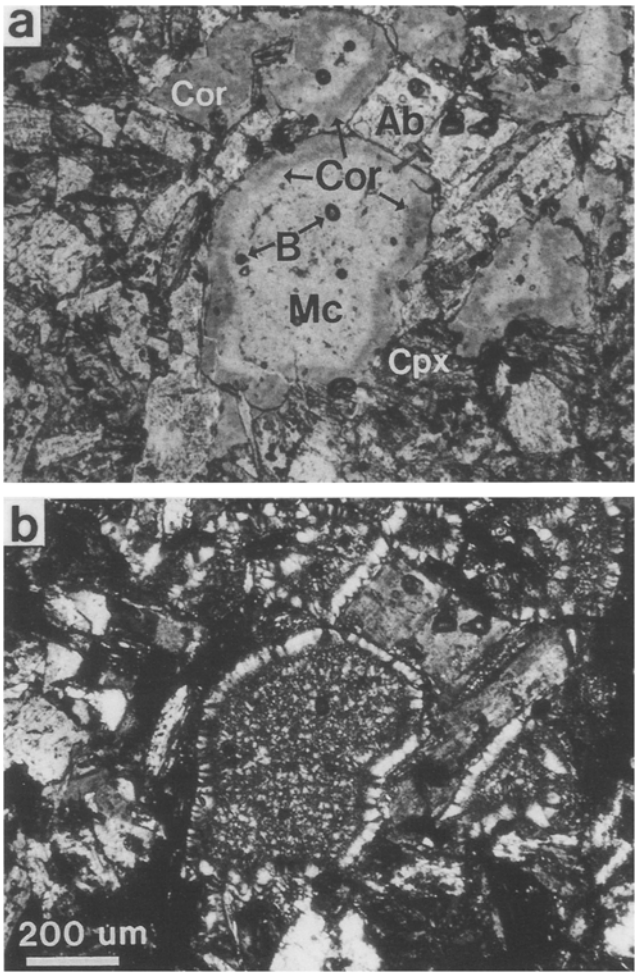

Fig. 2a, b. Photomicrographs showing the textures of rim and core chloritic minerals in amygdules of metabasalt from Junghua, northern Taiwan. **a** Plane-polarized light. Corrensite has a deeper yellowish color than mixed-layer chlorite($\sim$0.75)/corrensite. **b** Crossed nicols. *Ab*, Albite; *Mc*, mixed-layer chlorite/corrensite; *Cor*, corrensite; *Cpx*, clinopyroxene; *B*, air bubble

Fe), synthetic fayalite (Fe), muscovite (K, Al), rhodonite (Mn, Fe, Ca), and sphene (Ti, Ca), that had been ion-milled with the same procedures as the rock specimens.

Chemical compositions of the chloritic minerals were also obtained with a Cameca CAMEBAX electron microprobe using 15 kV and 10 nA beam current and Tiburon albite (Na), Gotthard K-feldspar (K), Broken Hill rhodonite (Mn), labradorite (Si, Ca) synthetic enstatite (Mg) and synthetic ferrosilite (Fe) as standards. The ZAF corrections were obtained with Cameca programs.

Oriented aggregates of the <2 μm fractions of air-dried, glycerol-treated, and heated (500° C, 1.5 h) samples were prepared for X-ray diffraction analysis. Small fragments of purified chloritic specimens picked separately by hand from the core and rim of an amygdule or interstitial space were analyzed using a Gandolfi camera. These samples were also separately treated with glycerol. All XRD analyses were obtained using CuKα radiation.

Geological setting and petrography

The metabasalt was collected from a 12-m-thick unit, accompanied by a lower unit of lapilli tuff and an upper unit of vitric-crystal tuff, that was intercalated within Oligocene pelitic rocks (Shau and Yang 1987). These rocks, constituting the Hsuehshan Range of Taiwan, have been subjected to regional metamorphism corresponding to zeolite facies to prehnite-pumpellyite facies conditions at $P=2$–3 kb and $T=220$–300° C (Chen et al. 1983; Shau and Yang 1987; Yang and Shau 1988). The metabasalt is located near Junghua, Taoyuanhsien, northern Taiwan, in the vicinity of the Northern Cross-Island Highway (Fig. 1). The locality is on the western side of the Hsuehshan Range, and the grade of metamorphism generally increases toward the east (Chen et al. 1983). The temperature of metamorphism around the Junghua area was at the lower end of the above temperature range, and was approximately 220° C (Shau and Yang 1987). The metabasalt was described as a diabase unit by Shau and Yang (1987) on the basis of texture. Because the name diabase has generally been used for intrusive rocks, the term "basalt" is used instead of "diabase" to emphasize its eruptive origin.

The main constituents of this metabasalt are albite, clinopyroxene, chloritic minerals, and lesser amounts of relict Fe-Ti oxides, sphene, calcite and quartz. Fibrous or rosette-like arrays of chloritic minerals occur in spaces between grains of albite and clinopyroxene and in amygdules. There is a clear difference in texture between rim and core materials (Fig. 2). Crystals of these chloritic minerals are usually several μm in length (or diameter) and <1 μm in thickness. Yellowish-green, platy corrensite occurs along the inner wall of amygdules and spaces between crystals of albite and clinopyroxene, forming a rim with (001) planes nearly perpendicular to the wall (the TEM results described below show that these rim materials contain some packets of chlorite layers), while pale green mixed-layer chlorite/corrensite with random orientation occurs as layered or rosette-like aggregates in the core (Fig. 2). This occurrence of corrensite is very similar to that of authigenic corrensite filling pore space in volcanoclastic sandstone from the Horsethief Formation, Montana (Almon et al. 1976). The chloritic minerals from both rim and core in the Junghua metabasalt are length-slow, indicating that their optic signs are negative (the grain size is too small for direct measurement of the optic sign), and they display very weak pleochroism. The rim corrensite has lower refractive indices but slightly higher birefringence than the mixed-layer chlorite/corrensite in the core (interference colors are pale yellow and grey, respectively). Chloritic minerals separated from the amygdules have refractive indices $\beta=1.610\pm0.002$ for core materials, and $\beta=1.598\pm0.004$ for rim materials. These optical properties deviate from normal optical properties of chlorites as discussed below.

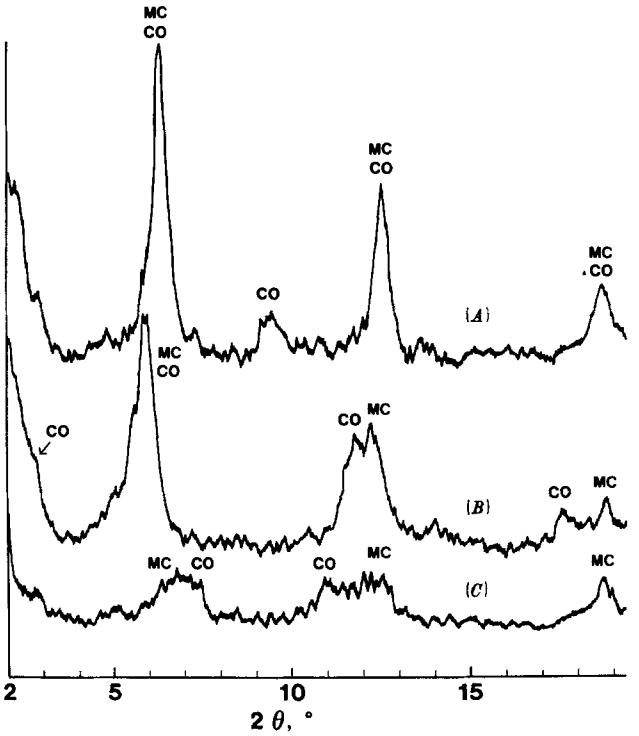

Fig. 3. XRD patterns of the <2 μm fraction of the Junghua metabasalt: air dried (*A*); glycerol treated (*B*); heated at 500° C for 1.5 h (*C*). The samples contain mixed-layer chlorite/corrensite (*MC*) and corrensite (*CO*)

XRD analyses

Diffractometer patterns of clay separates are shown in Fig. 3. The 7 Å reflection of air-dried chlorite is usually more intense than the 14 Å reflection. The intense 14 Å peak of the air-dried specimen from the Junghua metabasalt therefore implies that there may be a smectite- or vermiculite-like component. The shoulder on the sloping background at 2–3° (2Θ) is also compatible with the presence of mixed-layered phases.

After glycerol treatment (Fig. 3, pattern B), the 14 Å peak shifted to ~15 Å, became broader, and gained a tail on the low-angle side; a peak with $d=9.3$ Å (interpreted as 003 of corrensite) was no longer present. The 7 Å peak separated into 7 Å and 7.5 Å peaks, corresponding to 002 of chlorite and 004 of corrensite, respectively. A small peak with $d=5.1$ Å corresponds to the 006 reflection of corrensite.

Heat treatment at 500° C for 1.5 h caused a significant decrease in the intensity of peaks and resulted in two plateaus with spacings ranging from 11.9 to 13.8 Å and 7.1 to 8.0 Å, respectively (Fig. 3, pattern C). The pattern is similar to that of random mixed-layer chlorite/smectite plus chlorite described by Bettison and Schiffman (1988). However, the broad plateaus here are interpreted as consisting of 001 (~13.8 Å) and 002 (~7 Å) of mixed-layer chlorite/corrensite primarily from the core material, and 002 (~12 Å) and 003 (~8 Å) of collapsed corrensite from the rim material.

Separated rim and core materials analyzed using the Gandolfi camera give reflections that are more easily distinguished (Table 1). The patterns of non-treated specimens from core and rim have $I_{(14\,Å)} > I_{(7\,Å)}$, but the ratio $I_{(14\,Å)}/I_{(7\,Å)}$ of the rim material is larger than that of the core material. This indicates there is a greater smectite- or vermiculite-like component in the rim material. The core material generally gives a single series of $00l$ ($d_{001}=14$ Å) reflections, while the rim material has a series of $00l$ ($d_{001}=14$ Å) reflections plus extra reflections that apparently are derived from a series with $d_{001}=28$ Å (e.g., reflections with $d=9.4$ and 4.8 Å). The 060 reflections from both core and rim have $d=1.53$ to 1.55 Å, indicating that these chloritic minerals are trioctahedral phyllosilicates.

After glycerol treatment, the core material displays some expansion from 14.1 to 14.7 Å, while the rim material apparently consists of one less expandable phase

Table 1. X-ray diffraction data for mixed-layer chlorite/corrensite and corrensite from the Junghua metabasalt, northern Taiwan, obtained with a 114.6 mm diameter Gandolfi camera and Cu Kα(Ni) radiation

Mixed-layer chlorite/corrensite from an amygdule core

Air-dried		Glycerolated		*hkl*
d	*I*	*d*	*I*	
14.1	s	14.7	s	001
7.15	ms	7.36	s, b	002
4.65	w, b	4.63	m	020
3.57	m	3.55	m, b	004
2.87	vw	2.82	vw	005
2.60	w, b	2.60	w	131
2.47	w	2.51	w	132, 201
2.42	vw	2.43	vw	
2.29	vw	2.14	vw, b	
2.02	vw	2.02	vw, b	
1.549	m	1.549	m	060
1.518	vw	1.516	w	

Corrensite + mixed-layer chlorite/corrensite from an amygdule rim

Air-dried		*hkl*		Glycerolated		*hkl*	
d	*I*	Cor	Mcc	*d*	*I*	Cor	Mcc
13.9	vs	002	001	15.0	vs	002	001
9.48	vw	003					
				7.69	m	004	
7.12	s	004	002	7.17	m		002
4.81	vw	006	003	5.10	vw	006	
4.60	w	020	020	4.60	w	020	020
3.54	w, b	008	004	3.54	w		004
				3.44	w	009	
				2.83	vw	0011	005
2.58	w, b	131	131	2.60	w	131	131
				2.55	w		
2.46	w			2.45	w		
2.27	vw			2.27	vw		
2.00	vw			2.02	vw		
1.545	s	060	060	1.544	m	060	060
1.512	vw			1.510	vw		

Cor, Corrensite; Mcc, mixed-layer chlorite/corrensite; vs, very strong; s, strong; ms, moderately strong; m, moderate; w, weak; vw, very weak; b, broad or diffuse

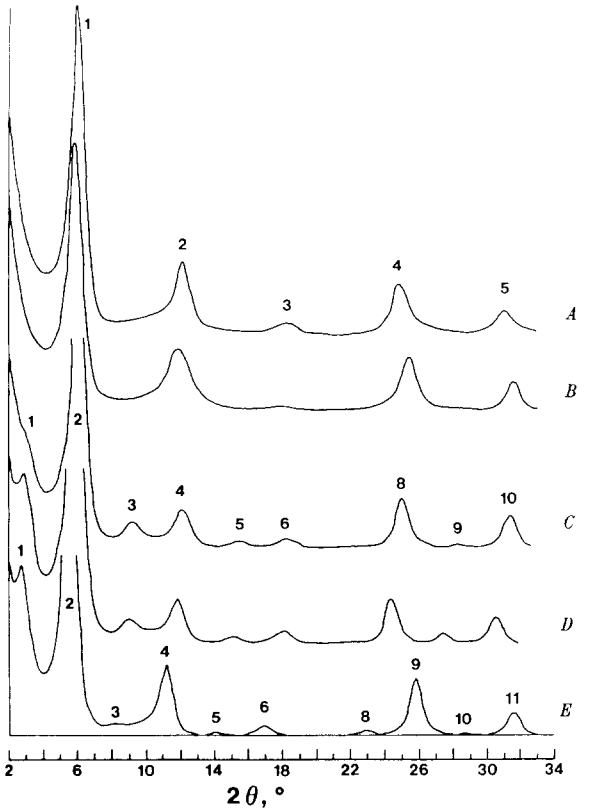

Fig. 4. Calculated XRD patterns of mixed-layer chlorite(0.75)/corrensite (*A* and *B*) and corrensite (*C–D*): chlorite(0.8)/smectite (*A*); chlorite(0.8)/smectite, glycerol treated (*B*); chlorite(0.5)/vermiculite (*C*); chlorite(0.5)/smectite (*D*); chlorite(0.5)/smectite, glycerol treated (*E*). All calculated with $R=1$ and $N=3$ to 9. The numbers are the indices for 00*l* reflections

(similar to the core material) and one more expandable phase (corrensite) which expands from 28 to 31 Å (estimated from high order reflections). The more expandable phase is therefore an ordered 1:1 mixed-layer chlorite/"expandable layers" with the expandable layers expanding from ~14 to ~17 Å after glycerolation. The XRD patterns of mixed-layer chlorite(0.8)/smectite ($R=1$) and ordered chlorite(0.5)/vermiculite and chlorite(0.5)/smectite calculated with the computer program NEWMOD (Reynolds 1985) are generally consistent with the experimental data (Fig. 4; cf. Table 1 and Fig. 3).

Microprobe analyses

Microprobe analyses of chloritic minerals from the rim and core of amygdules or intercrystal space are listed in Table 2. To facilitate comparison with the compositions of chlorite or chloritic minerals, normalization was based on 14 oxygen atoms (cf. Laird 1988). The rim chloritic minerals show a large variation of $\delta Al = 0.44$–0.76 ($\delta Al = Al^{VI} - Al^{IV}$ per formula unit), while Si/(Si + Al) varies from 0.68 to 0.72 and Fe/(Fe + Mg) from 0.35 to 0.39. The core chloritic minerals have lower but also variable δAl (0.26–0.44), and Si/(Si + Al) and Fe/(Fe + Mg) ratios of 0.65–0.67 and 0.39–0.40, respectively. The large excess of Al^{VI} relative to Al^{IV} requires apparent vacancies (ranging from 0.13 to 0.38) in octahedral sites when normalization is based on 14 oxygen atoms. This is a common feature in chlorite analyses from low-grade rocks (e.g., Boles and Coombs 1977; Cathelineau and Nieva 1985; Aguirre and Atherton 1987).

The rim material has much higher δAl, slightly higher Si/(Si + Al) and slightly lower Fe/(Fe + Mg) ratios relative to the core material. The total Ca + Na + K per formula is higher in the rim than in the core chloritic materials. The significant Ca content and smaller Na and K concentrations in these chloritic minerals are typical of samples with corrensite or smectite components.

TEM/AEM analyses

Areas exhibiting rim and core chloritic minerals were selected for TEM/AEM analysis. The TEM images (Fig. 5) show that the chloritic minerals are generally composed of stacks of many packets of layers, each packet several hundred Å in thickness (the term packet as used here defines a sequence of coherent layers with identical crystallographic orientation). The 00*l* lattice fringe images of the core material (Fig. 6) generally show 14 Å periodicity but always have some intercalated layers with 10 Å spacings. Such features resemble chlorite with some missing interlayer hydroxide (or "brucite") sheets. The combined TEM, XRD and analytical data (see below and Discussion) imply that the 14 Å fringes correspond to chlorite layers and the 10 Å fringes to collapsed smectite-like layers. Such collapse may be caused by dehydration in the high vacuum of the electron microscope (cf. Klimentidis and Mackinnon 1986). The smectite-like layers comprise approximately 20% of the total number of layers. Two or more adjacent 10 Å layers have not been observed. According to the nomenclature of Reynolds (1980, 1988), this chloritic material is apparently an $R=1$ chlorite(~0.8)/smectite, which is equivalent to a random interstratification of corrensite layers with excess chlorite layers ($R=0$ chlorite(~0.75)/corrensite). However, as two or three layers of 24 Å (14 + 10 Å) periodicity adjacent to each other were commonly observed, indicating a tendency of segregation of corrensite layers (Fig. 6), the stacking sequence of mixed-layer chlorite/corrensite is not completely random.

The TEM 00*l* lattice fringe images (Fig. 7) of the rim material generally show two kinds of materials that are intergrown as subparallel or parallel packets of layers. The more abundant type is dominated by layers of 24 Å periodicity but with some extra 14 Å layers. The less abundant type is dominated by layers with 14 Å periodicity but with some 24 Å corrensite layers although small packets may contain no corrensite layers (Fig. 7). The latter is similar to the mixed-layer chlorite/corrensite of the core material. However, the proportion of chlorite layers relative to corrensite layers is more variable within packets than that in the core. Corrensite packets of completely ordered 24 Å periodicity can be up to 1000 Å in thickness (Fig. 8). The SAED patterns of the core materials may show rational 14/n Å ($n=1, 2, \ldots$) reflections

Table 2. Microprobe analyses of mixed-layer chlorite/corrensite from amygdule cores and corrensite ± mixed-layer chlorite/corrensite from the rims of amygdules in the Junghua metabasalt, northern Taiwan

Wt%	Core material			Rim material		
	1	2	3	4	5	6
SiO_2	32.0 (5)[a]	32.9 (5)	34.1 (5)	33.9 (5)	37.1 (5)	35.5 (5)
Al_2O_3	14.4 (2)	14.5 (2)	14.3 (2)	13.4 (2)	12.7 (2)	13.7 (2)
FeO[b]	22.6 (7)	21.9 (7)	21.9 (7)	19.7 (6)	18.9 (6)	19.0 (6)
MgO	19.1 (3)	18.8 (3)	19.3 (3)	20.1 (3)	19.8 (3)	18.8 (3)
MnO	0.26 (5)	0.18 (4)	0.12 (2)	0.15 (3)	0.20 (4)	0.04 (1)
CaO	0.23 (2)	0.13 (2)	0.26 (3)	0.45 (4)	0.33 (3)	0.43 (4)
Na_2O	0.04 (1)	0.04 (1)	0.05 (1)	0.10 (1)	0.08 (1)	0.08 (1)
K_2O	0.01 (<1)	–	0.07 (1)	0.03 (<1)	0.04 (1)	0.07 (1)
Subtotal	88.7	88.5	90.2	87.8	89.1	87.6
No. of cations on the basis of 14 O						
Si	3.26 (5)	3.34 (5)	3.38 (5)	3.43 (5)	3.65 (5)	3.55 (5)
Al^{IV}	0.74 (1)	0.66 (1)	0.62 (1)	0.58 (1)	0.35 (1)	0.45 (1)
Al^{VI}	0.99 (1)	1.07 (2)	1.06 (1)	1.02 (1)	1.11 (2)	1.17 (2)
Fe^{2+}	1.93 (6)	1.86 (6)	1.82 (6)	1.67 (5)	1.56 (5)	1.59 (5)
Mg	2.90 (4)	2.84 (4)	2.85 (4)	3.02 (4)	2.89 (4)	2.81 (4)
Mn	0.022 (4)	0.015 (3)	0.010 (2)	0.013 (3)	0.016 (3)	0.003 (1)
Ca	0.025 (3)	0.015 (2)	0.027 (3)	0.048 (4)	0.034 (3)	0.047 (4)
Na	0.008 (1)	0.008 (1)	0.010 (1)	0.020 (2)	0.016 (2)	0.016 (2)
K	0.002	–	0.008 (1)	0.004 (1)	0.005 (1)	0.009 (1)
Total	9.88	9.80	9.79	9.79	9.63	9.65
Si/(Si+Al)	0.65 (2)	0.66 (2)	0.67 (2)	0.68 (2)	0.71 (2)	0.69 (2)
Fe/(Fe+Mg)	0.40 (2)	0.40 (2)	0.39 (2)	0.36 (2)	0.35 (2)	0.36 (2)
$Al^{VI}-Al^{IV}$	0.26 (2)	0.41 (3)	0.44 (2)	0.44 (2)	0.76 (3)	0.72 (3)
Ca+Na+K	0.04 (1)	0.02 (1)	0.05 (1)	0.07 (1)	0.06 (1)	0.07 (1)

[a] Numbers in parentheses are two standard deviations derived from counting statistics
[b] Total Fe as FeO

(Fig. 9a) or irrational reflections (Fig. 9b) depending on whether the selected area includes packets of nearly pure chlorite layers or chlorite plus corrensite layers. The SAED patterns of the corrensite-dominated area in the rim (Fig. 9c) always show more intense reflections with indices 001, 002, 003, 005, 007, 008, 00$\underline{10}$ and weaker reflections with $l=1+5n$ (except 001) and $l=4+5n$ ($n=1, 2, \ldots$).

The AEM chemical analyses were obtained in scanning mode by rastering the electron beam over thin edges with raster widths ranging from 200 to 500 Å. Analyses of three types of packets were obtained: (1) nearly pure chlorite having rational 14 Å reflections, (2) mixed-layer chlorite/corrensite packets with irrational reflections, or mixtures of mixed-layer chlorite/corrensite and corrensite, and (3) nearly pure corrensite packets having well-defined rational reflections with $d=24/n$ Å. The compositions expressed in normalized molar values as obtained using experimentally determined k values from standards are listed in Table 3 and plotted in Fig. 10. The Al and Fe contents of nearly pure chlorite are significantly higher and the Ca content much lower than those in mixed-layer chlorite/corrensite and corrensite. The Mn content is generally higher in chlorite than in corrensite. The corrensite formula is normalized to 14 oxygen atoms (chlorite formula) and 25 oxygen atoms (corrensite formula). The high values of δAl and numbers of vacancies for corrensite when normalized to a chlorite formula illustrate the effect of corrensite interlayers on bulk analyses of interlayered chloritic phases.

The AEM analyses are consistent with the microprobe results, except that the proportion of Ca is much higher in AEM analyses, clearly reflecting the compositional differences among chlorite, mixed-layer chlorite/corrensite, and corrensite. Assuming that the composition of packets having 14 Å rational reflections and the lowest value of δAl corresponds to ideal chlorite (analysis 1, Table 3), the chlorite formula (excluding Ca) is:

$$\underbrace{(Mg_{2.77}Fe_{2.18}Mn_{0.02}Al_{1.01})}_{5.98}\underbrace{(Si_{3.04}Al_{0.96})}_{4.00}O_{10}(OH)_8,$$

with an interlayer charge of about +1.0. This has been suggested as the most stable state for chlorite (Bailey 1988). Assuming that this chlorite composition contributes to half of the corrensite formula (e.g., analysis 7b, Table 3):

$$(Na_{<0.02}K_{<0.02}Ca_{0.18})\underbrace{(Mg_{5.07}Fe_{2.74}Mn_{0.02}Al_{1.17})}_{9.00}$$
$$\cdot\underbrace{(Si_{6.46}Al_{1.54})}_{8.00}O_{20}(OH)_{10}\cdot nH_2O,$$

Fig. 5. TEM bright field image of the amygdule core material showing that packets of mixed-layer chlorite/corrensite are 100 to 500 Å thick. Most layers are 14 Å chlorite layers but some interstratified 10 Å layers (collapsed smectite-like layers) create 24 Å corrensite layers (indicated by *arrows*). The outlined area is enlarged in Fig. 6

the other half, the smectite-like layers must, by difference, have the formula:

$$(Na_{<0.02}K_{<0.02}Ca_{0.18})\underbrace{(Mg_{2.30}Fe_{0.56}Al_{0.17})}_{3.03}\cdot\underbrace{(Si_{3.42}Al_{0.58})}_{4.00}O_{10}(OH)_2\cdot nH_2O$$

with Si/(Si + Al) = 0.82 and Fe/(Fe + Mg) = 0.20. The net negative charge per formula of the 2:1 layers of the "smectite" is approximately 0.4. This defines these expandable layers as smectite with a high charge rather than vermiculite, which has a layer charge greater than 0.6 (Bailey 1980, p. 98). The octahedral cation numbers are 5.98, 9.00 and 3.03 for the chlorite, corrensite and "smectite", respectively. These results are in excellent agreement with predicted values for trioctahedral phases and confirm that the chloritic phases in the Junghua metabasalt are all trioctahedral phyllosilicates, as implied by XRD data.

Figure 10a shows that the number of Si atoms per formula for different packets has a negative correlation with the Fe/(Fe + Mg) ratio. All formulae are normalized on the basis of the chlorite formula, 14 O. When the data are plotted as Fe/(Fe + Mg) vs. Si/(Si + Al) in order to avoid bias related to the method of normalization, they still show the same trend. Packets of nearly pure chlorite and corrensite have Fe/(Fe + Mg) ranging from 0.39 to 0.44, and from 0.34 to 0.36, respectively. Packets of mixed-layer chlorite/corrensite or mixtures of corrensite and chlorite/corrensite have Fe/(Fe + Mg) and Si values falling between those of the two end members.

The δAl values and the Ca content also have a negative correlation with Fe/(Fe + Mg) (Fig. 10b and 10c). Therefore, the decreasing Fe/(Fe + Mg) ratio and increasing amounts of Si, Ca and δAl for "chlorite" formulae correspond to increasing proportions of smectite-like layers in the direction of the corrensite end-member. The excess of Al^{VI} relative to Al^{IV} in "chlorite" thus provides a simple measure for estimating the proportion of interstratified smectite-like layers within chlorite layers.

Discussion

Summary of XRD and TEM/AEM results

The XRD and TEM/AEM data demonstrate that the chloritic minerals in the Junghua metabasalt are composed of two phases: (1) mixed-layer chlorite/corrensite which consists of interstratified layers of chlorite (ca. 75%) and corrensite (ca. 25%), occurring in the cores

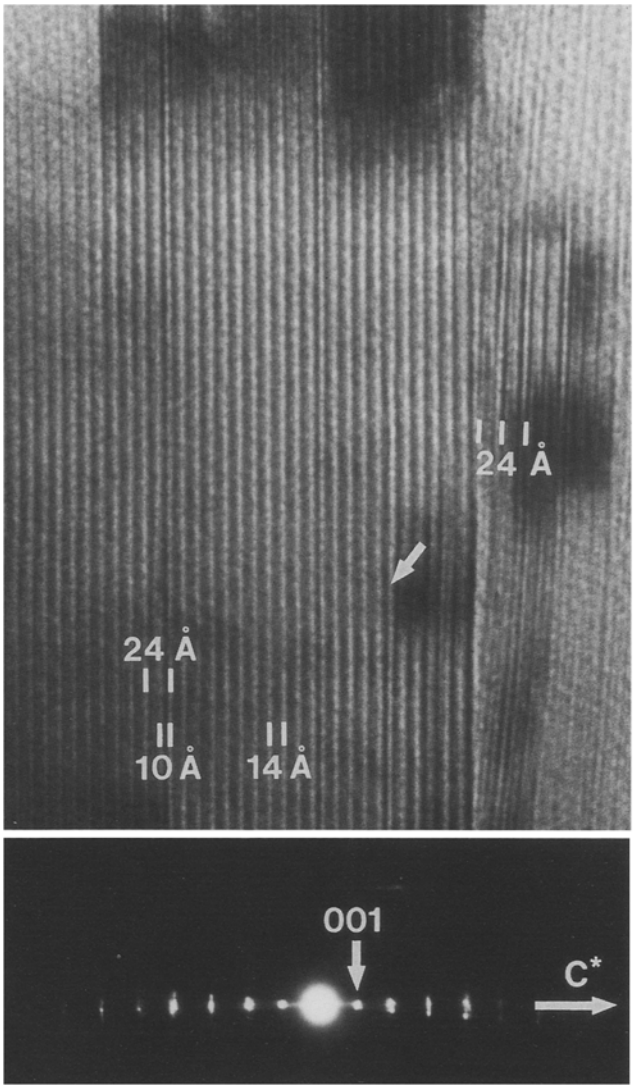

Fig. 6. TEM bright field lattice fringe image of (001) planes enlarged from the outlined area in Fig. 5. Layers with 10 Å spacing are interstratified within the dominant 14 Å layers but no two 10 Å layers are adjacent ($R=1$). The SAED pattern shows $00l$ reflections of a 14 Å phase but there is no evidence for the 10 Å phase in the diffraction pattern. The *arrow* points to transition of a 14 Å layer to a 10 Å layer

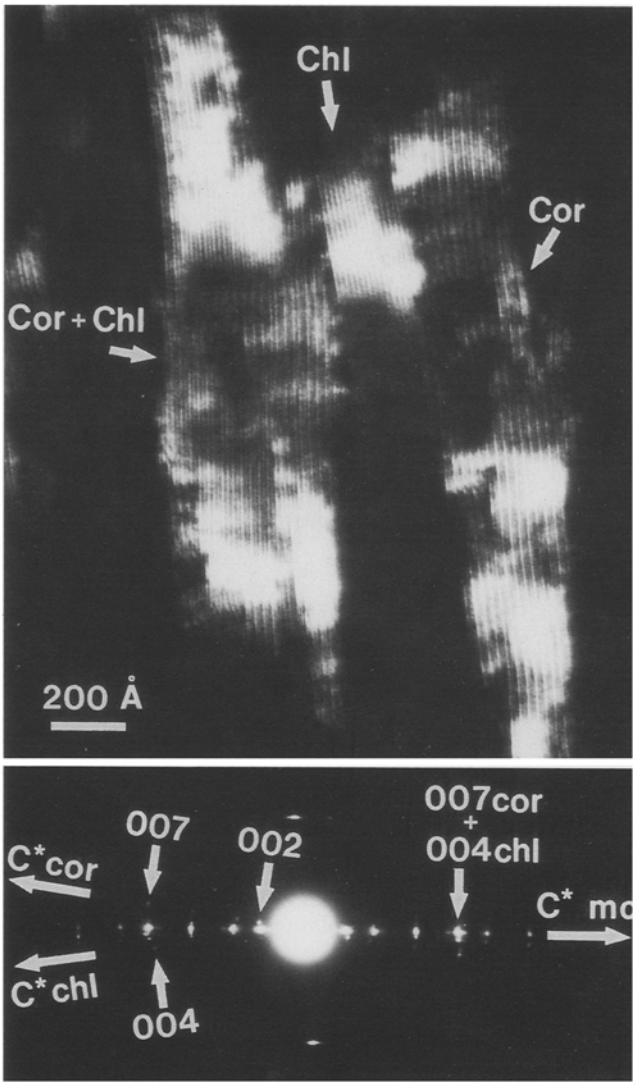

Fig. 7. TEM dark field lattice fringe image of (001) planes from the rim material, showing a small packet of pure chlorite (*Chl*) and packets of nearly pure corrensite (*Cor*) and chlorite/corrensite. The SAED pattern shows rational reflections of chlorite and corrensite, and irrational reflections of mixed-layer chlorite/corrensite (*mc*)

of amygdules and interstitial space, and (2) corrensite with lesser amounts of mixed-layer chlorite/corrensite occurring in the rims.

The mixed-layer chlorite/corrensite gives rise to irrational reflections that were observed in electron diffraction (Fig. 9b) and *X*-ray diffraction (Table 1). The ca. 25% corrensite layers (equivalent to 20% smectite-like layers) in the core material cause d_{001} of the glycerol-treated specimen to increase from 14.1 to 14.7 Å (Table 1), but it decreases only slightly ($\sim$13.8 Å) after heat-treatment at 500° C with no evidence of a phase having d_{001} of 10 Å. Because the smectite-like layers are never adjacent, as described in the following discussion, it is more sensible to describe this mixed-layered material as a mixed-layer chlorite(0.75)/corrensite rather than as an $R=1$ mixed-layer chlorite(0.8)/smectite. The stacking sequence of mixed-layer chlorite/corrensite is not completely random and it appears to have a tendency to segregate into chlorite and corrensite packets.

The coexisting packets of mixed-layer chlorite/corrensite, chlorite, and corrensite contain different proportions of Fe and Mg, in addition to different proportions of Al and Si. In Fig. 10a–10c, the increase in Si, δAl and Ca and decrease in Fe/(Fe+Mg) are correlated as a trend from nearly pure chlorite domains, through mixed-layer chlorite/corrensite or mixtures of chlorite/corrensite and corrensite, to corrensite packets. These data indicate that chlorite has higher values of Fe/(Fe+Mg) (0.39 to 0.44) than corrensite (0.34 to 0.36), and imply that chlorite layers and smectite-like layers have quite different Fe/(Fe+Mg) and Si/(Si+Al) ratios, even though they are intimately interstratified and/or

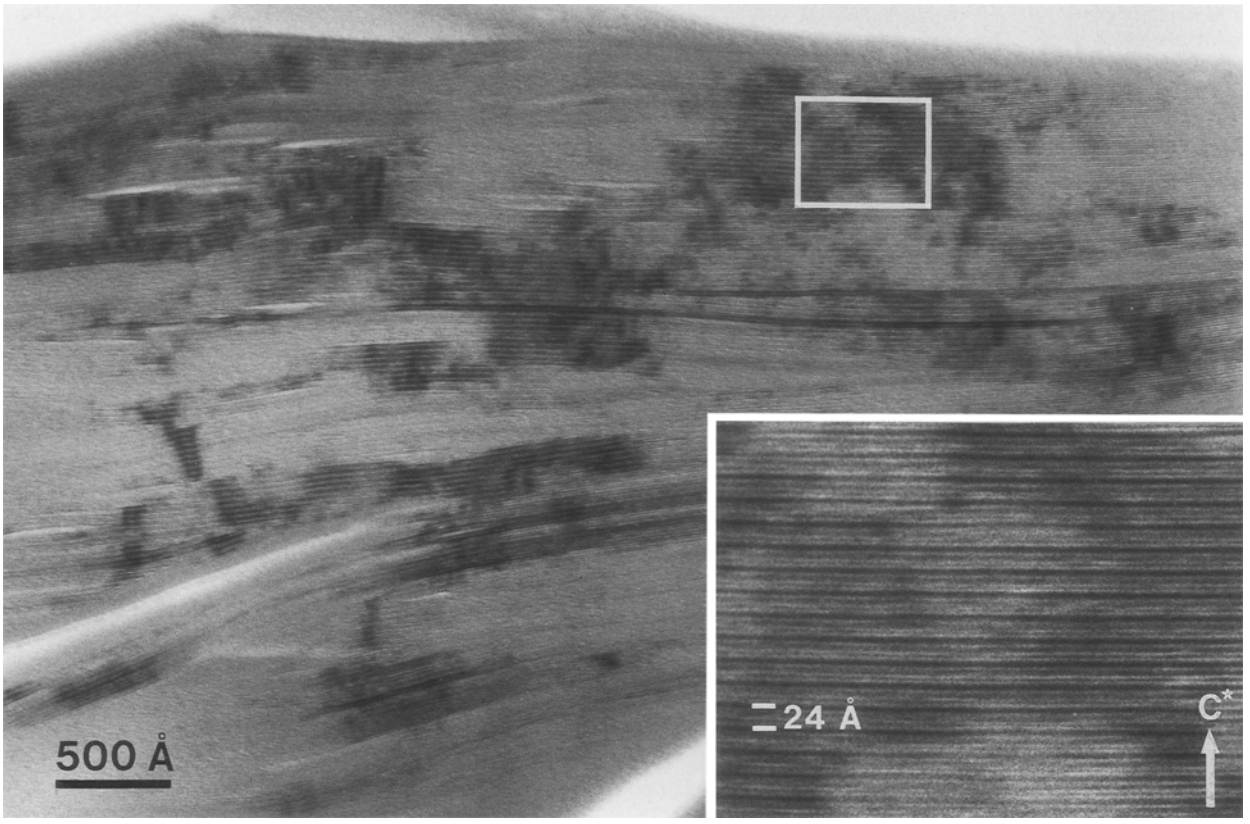

Fig. 8. TEM bright field lattice fringe image of (001) planes from the rim material shows that the layers with a periodicity of 24 Å (corrensite) are up to 1000 Å in thickness. The corresponding SAED pattern is shown in Fig. 9c

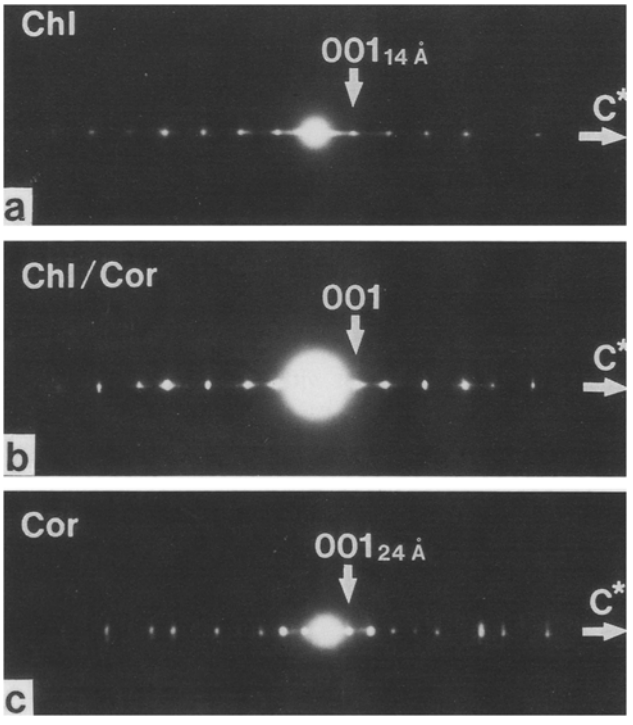

Fig. 9a–c. SAED patterns for (**a**) a nearly pure chlorite packet with rational 14/n Å reflections, (**b**) mixed-layer chlorite/corrensite packets with irrational reflections, and (**c**) a packet of corrensite with rational 24/n Å reflections

intergrown. The ratio Fe/(Fe + Mg) = 0.20 for the "smectite" component, as calculated by difference from the corrensite and chlorite, further emphasizes the differences in composition of octahedral sheets for the different structures.

In a review of the range of corrensite compositions, Brigatti and Poppi (1984b) suggested that "despite the chemical variability between corrensite, chlorite and saponite, corrensite appears chemically to be a well-defined species". The details of the composition of corrensite are a function of the detailed crystal structure relations, for which there are two distinctly different possibilities: (1) the structure consists of individual chlorite-like and smectite-like layers (expressed as $R = 1$ mixed-layer chlorite(0.5)/smectite tentatively), each of which retains the configurations of the individual phases, and for which the composition is an average of the two end-members, or (2) the structure of the 1:1 ordered phase is similar to, but has unique structure/crystal-chemical relations relative to the separate end-members, and therefore a unique composition range (cf. Newman and Brown 1987). The crystal-chemical relations for corrensite based on the second possibility are explored in detail in the following discussion.

Model of the crystal chemistry of the corrensite

The compositions of the mixed-layer chlorite/corrensite, corrensite and "smectite" indicate that a high proportion

Table 3. AEM analyses from 200–500 Å thick packets containing chlorite layers, chlorite plus corrensite layers (mixed-layer chlorite/corrensite), and corrensite layers, respectively, from the Junghua metabasalt, northern Taiwan

	1	2	3	4	5	6
Si	3.03 (3)[a]	3.12 (3)	3.13 (3)	3.44 (3)	3.33 (3)	3.34 (3)
Al^{IV}	0.97 (1)	0.88 (1)	0.87 (1)	0.56 (1)	0.67 (1)	0.66 (1)
Al^{VI}	0.99 (1)	0.98 (1)	1.00 (1)	1.05 (1)	0.94 (1)	0.98 (1)
Fe^{2+} [b]	2.17 (2)	2.00 (2)	2.09 (2)	1.75 (2)	1.88 (2)	1.91 (2)
Mg	2.76 (4)	2.91 (4)	2.79 (4)	2.88 (4)	2.97 (4)	2.87 (4)
Mn	0.016 (4)	0.015 (3)	0.021 (4)	0.014 (3)	0.017 (3)	0.016 (3)
Ca	0.049 (4)	0.040 (3)	0.044 (6)	0.070 (4)	0.054 (4)	0.064 (6)
K	n.d.	0.024 (4)	n.d.	n.d.	n.d.	n.d.
Total	9.99	9.95	9.94	9.76	9.86	9.84
Si/(Si+Al)	0.61 (1)	0.63 (1)	0.63 (1)	0.68 (1)	0.68 (1)	0.67 (1)
Fe/(Fe+Mg)	0.44 (1)	0.41 (1)	0.43 (1)	0.38 (1)	0.39 (1)	0.40 (1)
$Al^{VI}-Al^{IV}$	0.02 (2)	0.10 (2)	0.13 (2)	0.49 (2)	0.27 (2)	0.32 (2)
Ca+K	0.05	0.06 (1)	0.04 (1)	0.07	0.05	0.06 (1)

	7a	7b	8a	8b	9a	9b
Si	3.62 (3)	6.46 (5)	3.59 (3)	6.41 (5)	3.56 (3)	6.35 (5)
Al^{IV}	0.38 (1)	1.54 (3)	0.41 (1)	1.59 (3)	0.44 (1)	1.65 (3)
Al^{VI}	1.14 (2)	1.17 (2)	1.18 (2)	1.25 (2)	1.12 (2)	1.14 (2)
Fe^{2+} [b]	1.54 (2)	2.74 (4)	1.56 (2)	2.79 (4)	1.59 (2)	2.84 (4)
Mg	2.84 (3)	5.07 (5)	2.74 (3)	4.89 (5)	2.85 (3)	5.09 (5)
Mn	0.011 (3)	0.020 (5)	0.008 (3)	0.014 (5)	0.009 (3)	0.016 (5)
Ca	0.101 (5)	0.180 (9)	0.114 (5)	0.204 (9)	0.093 (4)	0.166 (7)
K	n.d.	n.d.	0.019 (4)	0.034 (7)	n.d.	n.d.
Total	9.63	17.18	9.62	17.17	9.66	17.26
Si/(Si+Al)	0.71 (1)	0.71 (1)	0.69 (1)	0.69 (1)	0.70 (1)	0.70 (1)
Fe/(Fe+Mg)	0.35 (1)	0.35 (1)	0.36 (1)	0.36 (1)	0.36 (1)	0.36 (1)
$Al^{VI}-Al^{IV}$	0.76 (3)	−0.37 (5)	0.77 (3)	−0.34 (5)	0.68 (3)	−0.51 (5)
Ca+K	0.10 (1)	0.18 (1)	0.13 (1)	0.23 (2)	0.09	0.17 (1)

1–3: Core material with rational 14/n Å SAED pattern (chlorite); 4–6: core material with irrational SAED pattern (mixed-layer chlorite/corrensite); 7–9: rim material with rational 24/n Å SAED pattern (corrensite). Analyses 1–6, 7a, 8a, and 9a are normalized on the basis of 14 O. Analyses 7b, 8b, and 9b are normalized on the basis of 25 O

[a] Numbers in parentheses are one standard deviation derived from counting statistics. ND, Not determined

[b] Total Fe as Fe^{2+}

of Al^{IV} substituting for Si in the tetrahedral sites of chlorite is accompanied by higher proportions of Fe^{2+} substituting for Mg in the octahedral sites of the 2:1 layers. Several authors have similarly shown that an increase in Al^{IV} correlates with an increase in octahedral Fe in chlorite (or chloritic minerals) from low-grade rocks (Kawachi 1975; Shirozu 1978; Kranidiotis and MacLean 1987; Bailey 1988; Nutt 1989). A simple and straightforward explanation for this trend concerns the misfit between octahedral and tetrahedral sheets. Substitution of Al^{IV} for Si causes an increase in size of the tetrahedral sheets. Substitution of the larger Fe^{2+} ion for Mg in the octahedral sheets gives rise to dilation of the octahedral sheet that compensates for the resultant misfit. Dallmeyer (1974) similarly proposed that Fe^{2+} substitutes preferentially, relative to Mg, in octahedral sites of biotite, when there is increased tetrahedral substitution of Al^{IV} for Si, and octahedral substitution of Al^{VI}, Ti, or Fe^{3+} for Mg and Fe^{2+}. Trioctahedral smectite is therefore expected to be Mg-rich and Fe-poor, given the requirement of minimum substitution of Al^{IV} for Si, while chlorite, having a range of Al^{IV}/Si, should accommodate a wide range of Fe/Mg, but with high Fe contents correlating with high Al^{IV}/Si. An extreme example with almost no Fe^{VI} and Al^{IV} is talc (J.M. Ferry, pers. comm.; Shau and Peacor 1989). That iron saponite (Fe-rich end-member trioctahedral smectite) is rare and unstable in nature and that Mg-rich saponite is common is thus expected (cf. Güven 1988).

Figure 11 shows schematic diagrams of the chlorite, corrensite and smectite structures, each labeled with the numbers of cations within each sheet. The tetrahedral site occupancies in corrensite are assumed to be symmetrical about the interlayers as consistent with a potential for ordering of the two kinds of interlayers, analogous with the model for the rectorite structure (Ahn and Peacor 1986; Newman and Brown 1987) and as suggested for corrensite by Reynolds (1988). Octahedral Al is as-

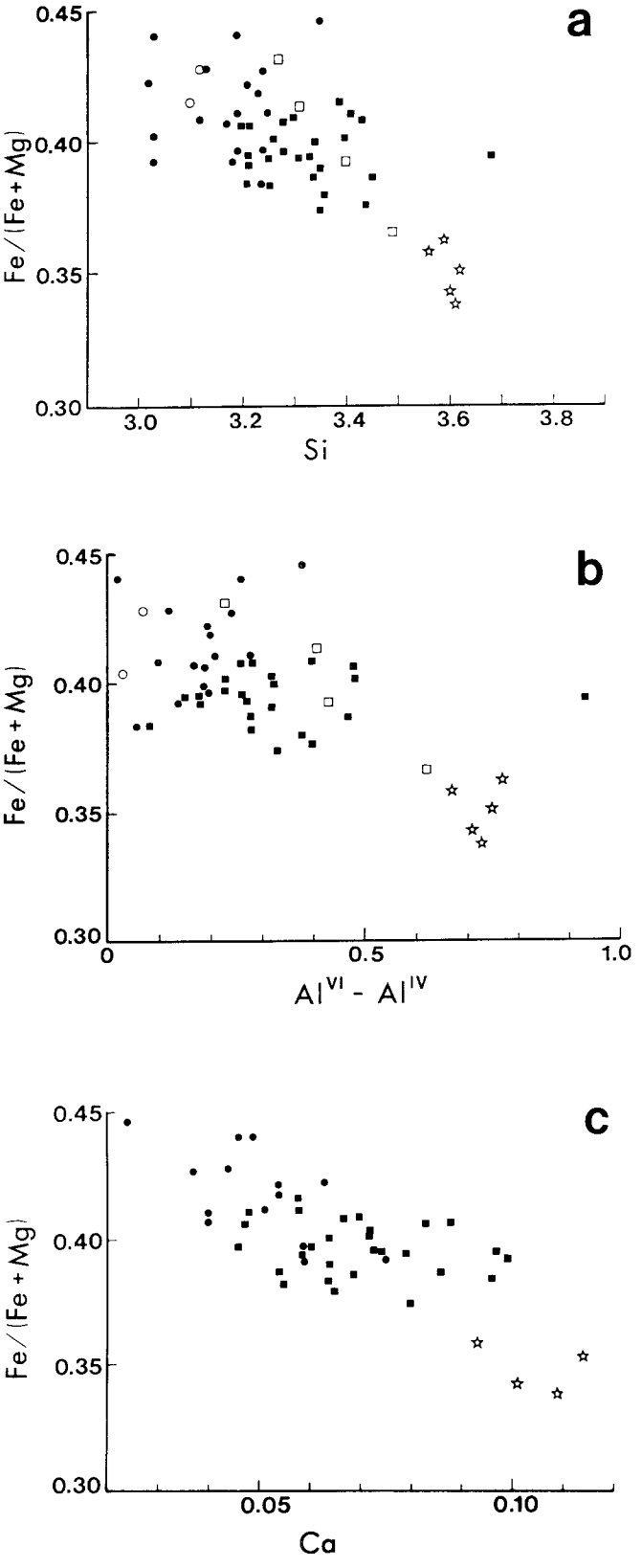

Fig. 10a–c. Compositions of the chloritic minerals in Junghua metabasalt obtained from AEM analyses in plots of Fe/(Fe+Mg) vs. Si (**a**), $Al^{VI}-Al^{IV}$ (**b**), and Ca (**c**). Total Fe as Fe^{2+}. *Solid symbols* and *open symbols* represent the core and rim materials of amygdules, respectively. *Circles*: chlorite packets with nearly rational reflections; *squares*: mixed-layer chlorite/corrensite packets with irrational reflections; *stars*: corrensite packets with rational reflections

sumed to be preferentially concentrated in the interlayer hydroxide sheet of chlorite since there is approximately 1.0 Al^{VI} per formula unit (cf. Bailey 1988). The Fe is assumed to be concentrated in the octahedral sheets within the 2:1 layers by analogy with the detailed structure of prochlorite (Steinfink 1958). Similar structure model for corrensite was also described by Reynolds (1988). However, corrensite was treated as a mixed-layer chlorite/smectite.

The corrensite structure model in which the Al^{IV}/Si distribution (tetrahedral charge) is symmetrical across the high-charge hydroxide interlayers and low-charge cation/H_2O-interlayers requires that the two tetrahedral sheets within a 2:1 layer must have distinctly different Si/Al^{IV} ratios (2.6 vs. 7, Fig. 11). The Fe/Mg ratios in each octahedral sheet within 2:1 layers of corrensite must be approximately the same since all octahedral sheets are similarly bounded by one high and one low charge tetrahedral sheet. The Fe/Mg ratio in such sheets must adjust to the dimensions and charge distribution of the bounding tetrahedral sheets. Therefore, chlorite, corrensite and smectite each should have unique Fe/Mg proportions in octahedral sheets of the 2:1 layers. The Fe/Mg ratios in octahedral sheets of the 2:1 layers are hypothesized to be 2.75, 0.93, and 0.27 for chlorite, corrensite, and smectite, respectively (Fig. 11) based on this model. If, on the other hand, Fe is assumed to be equally distributed into octahedral sheets and interlayer sheets of chlorite and corrensite (cf. Bailey 1988, Table 8), but with symmetry across interlayers retained, the corresponding Fe/Mg ratios in the octahedral sheets would be 0.58, 0.32, and 0.27 for chlorite, corrensite, and smectite, respectively.

In summary, corrensite has a unique Fe/Mg ratio relative to smectite and chlorite, as well as unique occupancy and geometry of tetrahedral sheets, assuming that the tetrahedral charge is symmetrical across the interlayers. Although the specific values of Fe/Mg in each octahedral sheet are not fixed (cf. Newman and Brown 1987), the Fe/Mg ratio will decrease on a relative basis from chlorite to corrensite to smectite.

Implications of the corrensite structure model for mixed-layer chlorite/corrensite or smectite/corrensite

For mixed-layer chlorite/corrensite as found in the cores of amygdules in the Junghua metabasalt, the two models for which corrensite is unique or for which the sequence of layers is considered to be an $R=1$ mixed-layer chlorite/smectite will give rise to different characteristics of the interfaces between layers of chlorite and corrensite.

For example, the corrensite with the unique structure model described above can be considered to be a component of mixed-layered chloritic materials, as shown in Fig. 12a. This mixed-layer chlorite/corrensite consists of interstratified 28 Å corrensite layers and 14 Å chlorite layers. The interfaces between the two kinds of layers are seen to be interlayer hydroxide sheets which are adjacent to two identical high-charge tetrahedral sheets. All

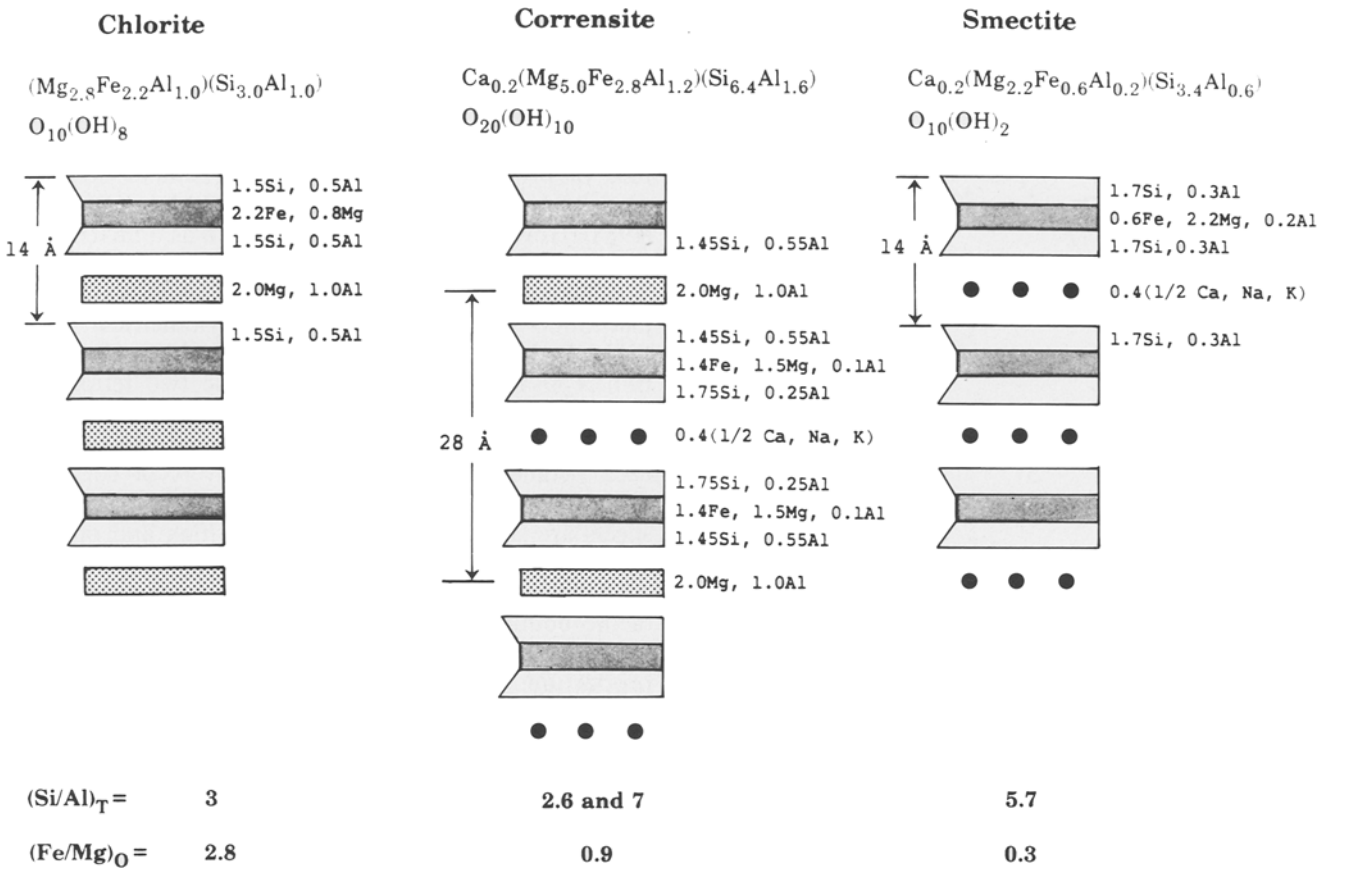

Fig. 11. Schematic structural models showing layer structures and distributions of elements in *chlorite*, *corrensite*, and *smectite*. The corrensite structure is considered to have tetrahedral charges symmetrical across the interlayer hydroxide sheets and interlayer cations. The H_2O contents of corrensite and smectite are not shown

such interfaces between chlorite and corrensite layers are identical irrespective of the proportion of chlorite layers relative to corrensite layers and/or their stacking sequence. In a similar way, smectite layers may be interstratified with corrensite layers, and the model requiring symmetry across interlayer cations provides identical low-charge interfaces between smectite and corrensite layers (Fig. 12b).

If, on the other hand, mixed-layer chlorite/corrensite is considered to consist of interstratified chlorite and smectite layers, i.e., $R=1$ chlorite/smectite, then tetrahedral charges are symmetrical across octahedral sheets and interlayers are bounded by both high- and low-charge tetrahedral sheets (i.e., this is the model for which corrensite is not unique). Thus, there would be two different types of interfaces, one high/low charge and the other high/high charge, between chlorite and "corrensite" layers. For a random ($R=0$) mixed-layer chlorite smectite (two or more smectite layers may be adjacent) the interfaces between chlorite and smectite layers can be treated either as hydroxide sheets or as interlayer cations. Both kinds of interfaces are bounded by both high- and low-charge tetrahedral sheets. This is an unsatisfactory state for hydroxide or cations/H_2O interlayers. The stacking sequence with chlorite (or smectite) and corrensite exhibiting identical interfaces with tetrahedral charge that is symmetrical across the interlayer (i.e., the model assuming a unique corrensite structure) is clearly more favorable than that for $R=1$ chlorite/smectite or $R=0$ chlorite/smectite. This in turn implies that the more stable assemblages should be considered to consist of mixed-layer chlorite/corrensite and/or smectite/corrensite plus discrete chlorite or smectite, rather than mixed-layer chlorite(x)/smectite ($0 \leq x \leq 1$) plus discrete phases. These tentative conclusions are supported by the fact that adjacent smectite-like layers have not been observed in both core and rim materials in the Junghua metabasalt, and by the general assemblages of chloritic minerals in other localities as described below.

Phase relations in natural occurrences

The structural/chemical model for corrensite described above emphasizes the uniqueness of the structure and composition of corrensite as compared with a model consisting of 1:1 ordered chlorite- and smectite-like layers. The existence of a unique chemistry and composition for corrensite implies that it represents a relatively stable phase, intermediate between chlorite and smectite; this in turn is consistent with the occurrence of each of the three phases chlorite, smectite and corrensite, or mixtures of them, rather than with a complete, continuous sequence of interstratified chlorite and smectite.

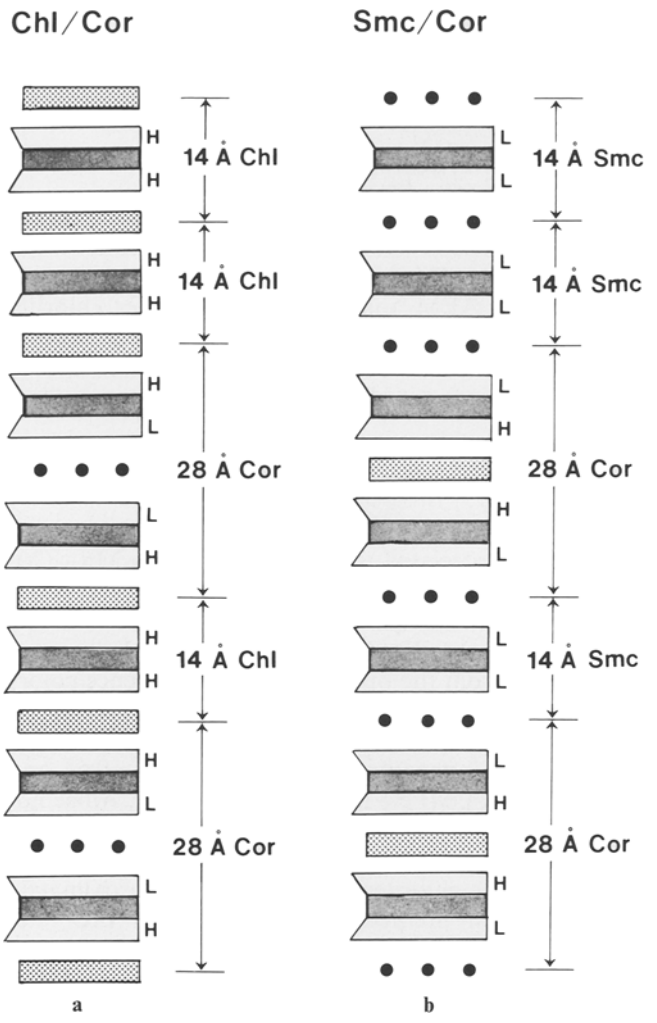

Fig. 12a, b. Schematic diagrams showing mixed-layer structures of (**a**) chlorite(>0.5)/corrensite and (**b**) smectite(>0.5)/corrensite. The 28 Å corrensite layer is considered to have tetrahedral charge symmetrical about the interlayer cations (low charge) or interlayer hydroxide sheets (high charge)

The phases observed in this study are in accord with such relations. The amygdule rims contain separate packets of layers of well-ordered corrensite and mixed-layer chlorite/corrensite, and occasionally tiny packets of nearly pure chlorite layers (Fig. 7). The material in the cores of amygdules is mixed-layer chlorite(~0.75)/corrensite with a tendency for corrensite layers to cluster together.

Similarly, Inoue et al. (1984) have shown that the percentage of expandable layers in mixed-layer chlorite/smectite decreases discontinuously from 100–80%, to 50–40%, to 15–10% as a function of increasing depth in a sequence of acidic pyroclastic sediments in the Ohyu District, Akita Prefecture, Japan. They emphasized the existence of gaps in the sequence between chlorite(0–0.2)/smectite and corrensite, and between corrensite and expandable chlorite (chlorite(0.85–0.9)/smectite). In addition, all three end-member phases coexist at intermediate depths. Those three phases are here inferred to be mixed-layer smectite/corrensite, corrensite, and mixed-layer chlorite/corrensite, respectively. Inoue et al. (1984) also indicated that corrensite layers that develop in smectite tend to occur as discrete packets and concluded that corrensite is a stable phase over a wide P-T range.

Additional observations in support of this relation come from the data of Brigatti and Poppi (1984a), who showed that corrensite commonly coexists with chlorite, with intermediate compositions not represented. The assemblage corrensite+smectite was also observed, but less frequently. In a study of the smectite-chlorite transition through diagenesis of clastic sediments in a Brazilian offshore basin, Chang et al. (1986) likewise showed that there is a gap between random smectite(0.8)/chlorite and ordered chlorite(0.6)/smectite ($R=1$) on the basis of plots of depth vs. percent chlorite in chlorite/smectite. They concluded that there was a continuous series between *ordered* chlorite(0.6)/smectite and *ordered* chlorite(0.9)/smectite. The end-members of that continuous series are more likely to be chlorite(0.3)/corrensite and chlorite(0.9)/corrensite since they are *ordered* mixed-layer phases. The intermediate compositions within the continuous series thus represent variable proportions of corrensite layers relative to chlorite layers.

The conclusion that chlorite, corrensite and smectite should occur as separate phases does not mean that they cannot occur as random mixed-layer chlorite/smectite. These phases typically form at low temperatures where disorder is the rule, and such disordered sequences can be expected to form under non-equilibrium conditions, and where kinetic factors favor the disordered phase (see below). For example, random mixed-layer chlorite/smectite has been described on the basis of XRD analysis (e.g., Evarts and Schiffman 1983; Alt et al. 1985; Bettison and Schiffman 1988). Random mixed-layer chlorite/smectite occurring in veinlets was found in a preliminary TEM study of hydrothermally altered oceanic basalts (Shau and Peacor 1989). However, Roberson (1987, 1988) has shown that some samples previously identified as random mixed-layer chlorite/smectite are physical mixtures of chlorite and corrensite on the basis of comparison of observed and calculated XRD patterns. The TEM studies of hydrothermally altered basalts from DSDP Hole 504B (Shau and Peacor 1988, 1989) are generally consistent with Roberson's observations.

It is the common occurrence of the separate, ordered phases (especially at higher temperatures) that establishes the phase relations, with the disordered phases being exceptions. Even in those phases that are identified by XRD as being randomly mixed-layered, there should still be a potential for clustering of corrensite units on the basis of the structure model, and TEM should be used whenever possible in order to provide unambiguous characterization of layer sequences.

Abnormal compositions of "chlorite" in low-grade rocks

Chemically anomalous chlorites that have excess Al^{VI} and significant amounts of Ca, Na, and/or K are very common in low-grade rocks. Several explanations have been proposed, among which are the following:

1. Vacancies in octahedral sites of chlorite (Foster 1962)
2. Oxygen ions replacing hydroxyl ions (Albee 1962)
3. Mixed-layering with other phyllosilicates:

a. Dioctahedral chlorites
b. Dioctahedral clay minerals, e.g., illite (Lee et al. 1984), dioctahedral smectite (Blatter et al. 1973), celadonite (Boles and Coombs 1975, 1977)
c. Trioctahedral clay minerals, e.g., trioctahedral smectite (Bettison and Schiffman 1988) or corrensite
d. Micas (Veblen 1983)
e. Talc (Schreyer et al. 1982)

4. Intimate intergrowth of submicron-sized chlorite with other phyllosilicates (discrete phases), e.g., white micas (Lee et al. 1984; White et al. 1985; Franceschelli et al. 1986; Shau et al. 1990), and corrensite.

The mixed-layer chlorite/corrensite of the present study exhibits typical chemical anomalies; indeed, they were chosen for study on that basis. The direct observation of interstratified corrensite layers (or trioctahedral smectite-like layers) within chlorite therefore directly correlates with the chemical anomalies.

The composition of the mixed-layer phase can be predicted on the basis of the proportions of the end-members. For example, if 80% chlorite layers having the ideal trioctahedral chlorite formula

$$(Mg_{2.5}Fe_{2.5}Al)(Si_3Al)O_{10}(OH)_8$$

are mixed with 20% trioctahedral 2:1 layers (e.g., smectite-like layers with lower Fe/(Fe + Mg) ratio),

$$M_{0.3}(Mg_{2.5}Fe_{0.5})(Si_{3.7}Al_{0.3})O_{10}(OH)_2 \cdot nH_2O$$
$$(M = \text{Na, K, or 1/2 Ca}),$$

the mixed-layer phase will have the formula

$$M_{0.06}(M_{2.5}Fe_{2.1}Al_{0.8})(Si_{3.14}Al_{0.86})O_{10}(OH)_{6.8} \cdot nH_2O.$$

If the compositions are normalized on the basis of 14 oxygen atoms in ideal chlorite, the Si will increase by a factor of 28/26.8 and the amount of Al^{IV} will decrease; the resulting formula will be

$$(M_{0.06}Mg_{2.61}Fe_{2.19}Al_{1.01})(Si_{3.28}Al_{0.72})O_{10}(OH)_8.$$

This yields an apparent value of $\delta Al = 0.29$.

Likewise, if there are 50% such smectite-like layers mixed with 50% chlorite layers, the Si of the mixed-layer phase will increase by a factor of 28/25 with an apparent value of $\delta Al = 0.79$ if the compositions are normalized to the chlorite formula (see Tables 2 and 3 for comparisons).

The specific compositions of chlorite and corrensite determined in the present study (Table 3) allow calculation of the formula of the smectite-like layers by subtraction of the chlorite composition from that of corrensite; the resulting formula is

$$(Na_{<0.02}K_{<0.02}Ca_{0.18})(Mg_{2.30}Fe_{0.56}Al_{2.18})$$
$$\cdot(Si_{3.42}Al_{0.58})O_{10}(OH)_2 \cdot nH_2O.$$

In accord with the observed proportions of layers in the mixed-layer chlorite/corrensite, 20% "smectite" and 80% chlorite give rise to the normalized "chlorite" formula

$$(Ca_{0.04}Mg_{2.80}Fe_{1.93}Mn_{0.17}Al_{1.06})$$
$$\cdot(Si_{3.25}Al_{0.75})O_{10}(OH)_8,$$

with $\delta Al = 0.31$, $Si/(Si + Al) = 0.64$, and $Fe/(Fe + Mg) = 0.41$. This is in good agreement with the microprobe and AEM analyses for mixed-layer chlorite/corrensite in the core of the amygdules (Tables 2, 3), and further confirms the relations between structure and chemistry of these mixed-layered phyllosilicates.

Abnormal optical properties of "chlorite" in low-grade rocks

Albee (1962) correlated the molar ratio (Fe + Mn + Cr)/(Fe + Mn + Cr + Mg) with refractive indices based on over 200 chlorite analyses (cf. Fig. 13). Based on Albee's scheme, the molar Fe/(Fe + Mg) ratio of chlorite may be estimated from the optic sign and interference colors or determined more accurately by measuring the β index of refraction. The optic sign is positive when $Fe/(Fe + Mg) < 0.52$, negative when $Fe/(Fe + Mg) > 0.52$, and $\beta = 1.630$ when $Fe/(Fe + Mg) = 0.52$. However, Albee noticed that chlorites from amygdules and veins in mafic igneous rocks exhibit large deviations from this trend. The anomalous chlorites have β indices approximately 0.011 less than predicted on the basis of their Fe/(Fe + Mg) values. They also have negative rather than the predicted positive optic signs. Albee also noted that molar Al^{VI} exceeds Al^{IV} in the anomalous chlorites. He suggested that the (apparent) extra positive charge is balanced by H vacancies and that the anomalous optic sign may be related to that.

Craw and Jamieson (1984) found that some chlorites from low-grade metavolcanic rocks have anomalous optical properties relative to Albee's (1962) scheme, i.e., such chlorites have negative optic signs and $Fe/(Fe + Mg) < 0.52$, but no apparent deviation of β indices from predicted values. They suggested that the anomalous optic signs were probably a result of metastable stacking sequences or polytypes of chlorite, and that the metastable polytypes would subsequently recrystallize to stable polytypes (e.g., IIb chlorite) with normal optics, as activated by a rise in temperature or application of stress.

The chloritic materials of this study have anomalous optics like those described by Albee (1962). The optic signs of both rim and core materials are negative, although the Fe/(Fe + Mg) ratios are compatible with positive signs. The β indices are 1.610 and 1.598 for the core and rim materials, respectively, values significantly less than predicted using Albee's data for chlorite. Because the negative deviation of β and the birefringence are greater in the rim material, and because that material has a higher proportion of smectite-like layers, the anomalous optics of chlorite are inferred to be due to mixed-layering of smectite- or vermiculite-like layers.

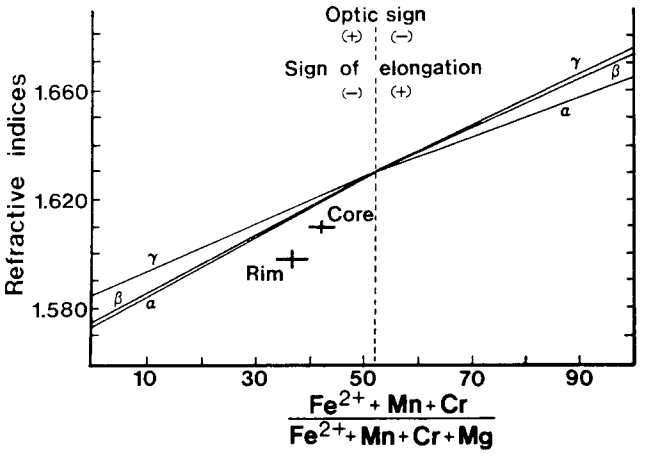

Fig. 13. Data for chloritic minerals from the Junghua metabasalt plotted in the diagram of Albee (1962) showing refractive indices vs. chemical composition of chlorite. Rim: corrensite ± mixed-layer chlorite/corrensite, core: mixed-layer chlorite/corrensite

In general, refractive index is dependent on density and polarizability (e.g., Bloss 1971, Chap. 12), and materials with larger density or polarizability have higher refractive indices. Compared with chlorite, smectite has much smaller polarizability in the direction perpendicular to the basal plane due to the larger distance and weak bonds between the 2:1 layers. The larger difference in polarizabilities between the direction perpendicular to the basal plane and that parallel to the basal plane causes the difference between indices α and γ ($\gamma \cong \beta$ and a negative optic sign for 2:1 layer phyllosilicates) to be larger for smectite, and therefore smectite always has higher birefringence than chlorite. Thus, if some smectite-like layers are interstratified within chlorite, they will strongly decrease the polarizability along the direction perpendicular to (001) and so decrease the refractive indices along that direction. This will cause γ (which is nearly perpendicular to (001) if the optic sign is positive) of the original chlorite (assuming $Fe/(Fe+Mg) < 0.52$) to become α in the mixed-layered structure and the optic sign will be changed from positive to negative. The lower $Fe/(Fe+Mg)$ ratio for smectite-like layers causes a decrease in all three indices of the mixed-layered phase. Greater proportions of smectite-like layers interstratified within chlorite will correlate directly with higher birefringence and smaller indices.

Figure 13 shows β indices versus $Fe/(Fe+Mg)$ of the rim and core chloritic minerals of the Junghua metabasalt plotted in Albee's scheme. The rim material, which consists primarily of corrensite (50% smectite-like layers) and lesser amounts of chlorite/corrensite (20% smectite-like layers) shows, as expected, lower index and higher birefringence than the core material which is primarily mixed-layer chlorite/corrensite. The negative deviations of the β indices from those of normal chlorites are 0.015 and 0.009 for rim and core materials respectively, and are consistent with the deviations (-0.011) of "chlorites" in altered mafic rocks observed by Albee (1962). The mixed-layering of smectite-like or vermiculite-like layers in chlorite is therefore the cause of anomalous optics in the chloritic materials of this study, and is most probably the cause in "chlorite" in low-grade mafic rocks from other localities. Albee's (1962) correlation scheme can be used for "true" chlorite (Black 1975; Craw and Jamieson 1984), and it provides a simple test of the presence or absence of interstratification of smectite- or vermiculite-like layers.

Effects of Fe/Mg, temperature and kinetics on the occurrence of chlorite and "mixed-layer chlorite/smectite"

Several authors have suggested relationships between trends in the composition of chlorite and factors such as metamorphic grade, bulk rock composition, fluid composition and reaction kinetics (e.g., Cathelineau and Nieva 1985; Shikazono and Kawahata 1987; Laird 1988).

"Chlorite" composition as a function of metamorphic grade. An increase in Mg content (decreasing Fe/(Fe+Mg)) of chlorite has generally been found to correlate with increasing metamorphic grade in low-grade metabasic rocks (e.g., Cooper 1972; Baltazis and Katagas 1984; Cho et al. 1986). Similarly, Leitch (1975) studied metabasic rocks in the Nambucca Slate Belt of northern New South Wales which range from prehnite-pumpellyite, to pumpellyite-actinolite, to greenschist facies. The Si/(Si+Al) ratios of chlorites were shown to decrease from 0.55 to 0.48, while the Fe/(Fe+Mg) ratios decreased from 0.41 to 0.22 with increasing metamorphic grade. The Si/(Si+Al) ratio in chlorite was also found to decrease with increasing metamorphic grade by Ernst et al. (1970) in Sanbagawa blueschist terranes.

In contrast with the general trend of increasing Al^{IV} with decreasing Fe/(Fe+Mg) shown by Leitch (1975), "chlorite" having high Al^{IV} correlated with high Fe/(Fe+Mg) from low-grade rocks has been described (e.g., Kawachi 1975; Shirozu 1978; Kranidiotis and MacLean 1987; Bailey 1988; Nutt 1989). However, this trend of increasing Al^{IV} (or decreasing Si/(Si+Al)) of so-called "chlorite" does not necessarily indicate that Al^{IV} and Fe contents of chlorite increase concomitantly, unless it is first shown that the normalized formulae have Al^{VI} (plus Fe^{3+}, if any) = Al^{IV} as consistent with pure chlorite. If interstratification of smectite-like or corrensite-like layers occurs, then there is a concomitant increase in Al^{IV}, and increase in Fe/(Fe+Mg), as shown above. If such trends occur in "chlorites" having $Al^{VI} > Al^{IV}$ then they are most certainly related to decreasing proportions of interstratified corrensite layers or smectite-like layers (Fig. 10a and 10b). Similar compositional variations of chloritic minerals related to varying proportions of interstratified trioctahedral and dioctahedral smectites have been observed by XRD in hydrothermally metamorphosed ophiolite samples (Evarts and Schiffman 1983). A general compositional change of the chlorite-smectite "intergrowth" from low Al and Fe/Mg in saponite-bearing rocks to high Al and Fe/Mg in saponite-free rocks with increasing grade of metamorphism in altered basalts was also reported by Ferry et al. (1987).

Cathelineau and Nieva (1985) proposed a chlorite geothermometer based on the Al^{IV} content of chlorite and temperature as estimated from observations of fluid inclusions, down-hole measurements, and chemical geothermometers in the Los Azufres (Mexico) geothermal system. The "chlorites" occurring in the hydrothermally altered andesite show a linear correlation between Al^{IV} (0.49–1.40) and estimated temperature (130–290° C) without a systematic change of Si/(Si+Al) and Fe/(Fe+Mg) ratios. However, the large excess of Al^{VI} (δAl ranges from 0.07 to 0.71 with decreasing temperature) and low but relatively constant Fe/(Fe+Mg) ratio (0.24–0.38) imply that most of those low-temperature "chlorites" may have interstratified corrensite or smectite-like layers, or more likely, phengite-illite layers as judged from their relatively invariable Si/(Si+Al) and Fe/(Fe+Mg) ratios. The increase of Al^{IV} in the "chlorite" formula would be a result of decreasing proportions of smectite-like or illite layers within chlorite and could be controlled in part by temperature. Likewise, the chlorite geothermometer based on a six-component chlorite solid solution model proposed by Walshe (1986) should be applied cautiously because most microprobe analyses of the "chlorites" that formed at lower temperatures ($< \sim 300°$ C) and used for calibration probably contain mixed-layered phases.

Strens et al. (1987) observed chlorites from six distinctive chlorite-quartz assemblages in central Borrowdale, Cumbria (UK) showing an apparent trend of increasing Fe/(Fe+Mg) in chlorites (0.46–0.84) with increasing temperatures (110–350° C). They inferred that the variations in Fe/(Fe+Mg) reflect the availability of iron in the veins rather than being a function of temperature. However, the negative correlation of Fe/(Fe+Mg) vs. Si (Strens et al. 1987, Fig. 3) and the abnormally low β indices compared to predicted values from Albee's (1962) scheme imply that the increasing Fe/(Fe+Mg) is correlated with decreasing proportions of interstratified clay minerals.

The apparent correlations of Fe and Si contents of "chlorite" with temperature and metamorphic grade are most likely related to mixed-layering of smectite-like and corrensite-like layers in chlorite, rather than being a function of the crystal chemistry of ideal chlorite. It is therefore essential that the absence of interstratification of such phases be verified by any one of several means suggested above, before such correlations can be attributed directly to chlorite. On the other hand, such correlations may be indirectly meaningful in that smectite is a phase consistent with lower temperatures than chlorite, and chemical correlations that measure changes in "chlorite" composition due to variable amounts of interstratified smectite-like layers may truly reflect changes in grade. Such variations must be treated with caution, as the occurrence of smectite-like interlayers may be related to kinetic factors, at least in part, rather than equilibrium functions.

Bulk rock chemical composition. Although the general relation of bulk rock composition to chlorite composition is well established (e.g., Albee 1962; Laird 1988), there is no general agreement as to how bulk rock composition would affect the proportions of chlorite, corrensite and smectite/vermiculite. Brigatti and Poppi (1984b) inferred that if Fe/(Fe+Mg)>0.5, chlorite alone is favored, but with increasing Mg, chlorite appears to be replaced by corrensite and trioctahedral smectite. Velde (1977) has suggested that corrensite tends to be more magnesian, and that chlorite is favored to form in rocks which are Fe^{2+}-rich, based on hydrothermal experiments. The high Fe/(Fe+Mg) ratio for mixed-layer chlorite/corrensite and the relatively low Fe/(Fe+Mg) value for corrensite in the Junghua metabasalt is therefore typical of other occurrences. This relation can be rationalized in terms of simple ad hoc crystal-chemical arguments as pointed out in an earlier section.

High bulk-rock Fe/Mg ratios favor the formation of Fe-rich chlorite that does not have significant compositional anomalies or expandable properties in low-grade metapelites or metagraywackes (e.g., Ernst et al. 1970; Shau et al. 1990) and in buried sedimentary rocks undergoing diagenesis (e.g., Ahn and Peacor 1985; Curtis et al. 1985; Pollastro 1988). Curtis et al. (1985) inferred from XRD studies that most of authigenic chlorites in sandstones are well-crystallized and their AEM analyses showed that Fe/(Fe+Mg) of chlorite ranged from 0.47 to 0.88, although slightly lower Fe/(Fe+Mg) ratios were also observed in some "swelling chlorites". Pollastro (1988) found authigenic, well-crystallized, Fe-rich chlorite in Simpson Group sandstones and shales. These examples indicate that for sedimentary rocks like sandstones or pelites which generally have high Fe/(Fe+Mg) as compared with mafic rocks, the formation of Fe-rich chlorite is promoted instead of smectite or corrensite even in the low temperature range of 150–250° C.

The ratio Fe/(Fe+Mg) and temperature are therefore both major factors in controlling the formation of chlorite and mixed-layer chlorite/smectite or corrensite. Smectite is favored by both low temperatures and low Fe/(Fe+Mg) ratios for the fluid or bulk rock; with an increase in temperature and Fe/(Fe+Mg) ratio, corrensite and then chlorite is favored. Not only is this true of the separate phases, but there will be equivalent trends in proportions of corrensite layers in both smectite and chlorite.

Kinetic factors and Ostwald-step-rule relations. Kinetic factors may also be significant in determining the structure and/or the composition of phases that form, especially at the lowest temperatures. For example, Lippmann (1979, 1981) has hypothesized that all clay minerals are metastable under surface or near-surface conditions, including conditions corresponding to diagenesis and metamorphism at temperatures below those of the greenschist facies. The phases observed in this study are prime examples of metastable phases, in that the heterogeneous structures (i.e., variety of mixed-layering occurring in closely associated packets) are direct evidence for a lack of chemical equilibrium. It is well known that, in accord with the Ostwald step rule, crystallization from solution at low temperatures generally gives rise to metastable phases that tend to react progressively through dissolution/crystallization steps toward equilibrium

states. Therefore, great care must be used in interpreting trends in either structure or composition of a given phase in terms of equilibrium relations.

In the case of the trioctahedral phases, there is evidence (Lippmann 1979, 1981) that smectite may be metastable relative to chlorite (plus other phases), with the occurrence of smectite being determined by kinetic factors rather than those relating to equilibrium conditions. Although the stable trioctahedral phyllosilicate at all temperatures may indeed be chlorite (Lippmann 1981), the metastable occurrence of phases containing smectite-like layers due to kinetic factors will still follow a predictable trend of increasing proportion of smectite with decreasing temperature, assuming that Mg concentration is sufficiently high. The general relationships among composition, structure and chemistry described above, although of an ad hoc qualitative nature, are in agreement with observed trends in structure and chemistry, and therefore must be significant for smectite (or vermiculite), corrensite and chlorite even though the phases may be metastable.

The first phases to form from solutions at the lowest temperatures may, as consistent with Ostwald's step rule, be disordered mixed-layer sequences consisting of smectite- and chlorite-like layers. In order of increasing stability, such phases would be replaced by mixed-layer chlorite/corrensite or smectite/corrensite, and then by separate phases, such as chlorite + corrensite or smectite + corrensite. Assuming that smectite-like layers are metastable at all temperatures, the final, stable phase would be chlorite. The above sequence would be observed in a burial metamorphic environment, with disordered interstratified phases occurring as the earliest phases at the lowest temperature. The sequence is consistent with the structure model for corrensite in that the model simply accounts for the formation of corrensite, but does not require that it be a stable phase in the strict thermodynamic sense.

Paragenesis of corrensite and mixed-layer chlorite/corrensite in the Junghua basalt

Both amygdules and interstitial space between albite and clinopyroxene grains show similar distributions of chloritic phases as rim and core patterns in the Junghua metabasalt (Fig. 2). Only mixed-layer chlorite/corrensite and corrensite fill both amygdules and interstitial space; that is, there are no other minerals such as Fe-Ti oxides, sphene and apatite, as would be expected if the chloritic minerals are replacements of interstitial matrix including glass or microlites. The interstitial space is therefore inferred to have been void space in the original fresh basalt (J.C. Alt, pers. comm.). Direct crystallization of the corrensite and mixed-layer chlorite/corrensite from solution in these void spaces without a phyllosilicate precursor is implied by the textures. Pore fluids are inferred to have saturated all pore space, and to have directly given rise first to precipitation of corrensite plus some mixed-layer chlorite/corrensite on the rims of void space, followed by crystallization of mixed-layer chlorite/corrensite in the cores. Because the relations imply that all chloritic materials formed over a limited range of temperature, the variable proportions of chlorite layers relative to corrensite layers in cores and rims are inferred to be primarily controlled by changing fluid composition.

Chloritic minerals in amygdaloidal basalts commonly show textures indicating chemical or structural zoning that universally appear to be similar to the same sequence as observed in the Junghua metabasalt; i.e., mixed-layer chlorite/expandable clay is dominant in rims and "chlorite" (a phase approaching ideal chlorite in structure) is dominant in cores. For example, Viereck et al. (1982) studied alteration of volcanoclastic rocks from the Reydarfjordur Drill Hole, eastern Iceland. They found that there is relative enrichment in Al in amygdaloidal "chlorite" from rim to core, although the opposite trend is infrequently observed. The rim "chlorite" with low Al content generally shows unusually high birefringence. These data imply that the rim material has a smectite or vermiculite (or corrensite) component. The large variations in composition of chlorites were inferred to have been caused by variable chemistry of mobile fluids (Viereck et al. 1982). Similar assemblages have also been found in pore-filling chloritic minerals in low-grade metasedimentary rocks. Boles and Coombs (1977) found that the pore-filling chloritic minerals from zeolite facies metasandstone in the Southland Syncline, New Zealand have higher birefringence and higher cation deficiencies in the rim, suggesting a higher content of interstratified smectite-like layers than in the later precipitated material which fills the cores of voids.

The temperature of formation of the corrensite and mixed-layer chlorite/corrensite in the Junghua metabasalt can be constrained by comparison with data from other occurrences, with due regard to the fact that "reaction progress" is probably being measured, rather than equilibrium temperature. The temperature for the first appearance of corrensite has been estimated as 90° C in Neogene sediments of Japan (Iijima and Utada 1971), 70° C in shales and 60° C in sandstones (Chang et al. 1986). As corrensite and chlorite coexist over a fairly large temperature range, the transition from mixed-layer chlorite/smectite to chlorite should be treated as the disappearance of corrensite. The temperature of the disappearance of corrensite has been reported to be 230–250° C in Icelandic geothermal fields (Kristmannsdóttir 1975, 1979), and approximately 225° C in the Del Puerto ophiolite (Evarts and Schiffman 1983). Variations in composition (or optical anomalies) of "chlorite" in many low-grade rocks may also be correlated with temperature to determine the relations to the proportions of "true" chlorite and corrensite layers. The disappearance of corrensite can be assumed to correspond to the development of normal chlorite compositions with nearly ideal structural formulae without excess of Al^{VI}. The temperature corresponding to the disappearance of corrensite or other expandable phases would therefore be 220–260° C in the Los Azufres geothermal system (cf. Cathelineau and Nieva 1985; Cathelineau and Izquierdo 1988).

The temperature of metamorphism of the Junghua metabasalt has been estimated as approximately 220° C (Chen et al. 1983; Shau and Yang 1987). The paragenesis of mixed-layer chlorite/corrensite and corrensite in the Junghua metabasalt is therefore consistent with the range of temperature of formation of coexisting corrensite and chlorite in other low-grade rocks.

Summary and conclusions

1. The chloritic minerals occurring in amygdules and other void spaces from the Junghua metabasalt, northern Taiwan have abnormal compositions and optics, and slightly expandable properties similar to many "chlorites" (including some so-called "swelling chlorite") in other low-grade mafic rocks. They consist of corrensite and mixed-layer chlorite($\sim$0.75)/corrensite.

2. Both chlorite layers and corrensite layers in the coexisting mixed-layer chlorite/corrensite and corrensite have unique compositions implying that the contents of Fe (relative to Mg) and Al^{IV} (relative to Si) decrease in the order of chlorite, corrensite, to smectite in response to unique crystal-chemical relations in each mineral.

3. A model for the corrensite crystal structure is consistent with the observed data and suggests that corrensite should be treated as a unique phase rather than as a 1:1 ordered mixed-layer chlorite/smectite. It also implies that the assemblages consisting of mixed-layer chlorite/corrensite and/or smectite/corrensite plus discrete chlorite, corrensite or smectite are more stable than those with random mixed-layer chlorite/smectite plus discrete phases.

4. The Al^{VI}/Al^{IV}, Si/(Si + Al) and Fe/(Fe + Mg) ratios, optical properties (e.g., β index), and expandability after glycerolation in mixed-layer chloritic minerals are correlated with the proportions of corrensite (or smectite-like) layers. Measurements of the above properties provide a simple test of the existence of mixed-layered components within chlorite.

5. Temperature, Fe/Mg ratio in bulk rock or fluid composition, and kinetic factors are inferred to have major effects on the occurrence of chlorite, corrensite, smectite, and their mixed-layered equivalents. Compositional variations of "chlorite" in low-grade rocks that appear to correlate with temperature or metamorphic grade more likely reflect the variable proportion of mixed-layered components in most cases.

Acknowledgements. We are grateful to Houng-Yi Yang for kindly providing the samples of metabasalt. We thank Herman E. Roberson and Wei-Teh Jiang for their many helpful discussions. We also thank the National Museum of Natural History, Smithsonian Institution for supplying the sphene standard (B20360). The assistance of Carl Henderson of the Electron Microbeam Analysis Laboratory of the University of Michigan is gratefully acknowledged. The manuscript was improved by the reviews of John M. Ferry and two anonymous reviewers. This study was supported by NSF Grants EAR-86-04170 and EAR-88-17080 to D.R. Peacor, and NSF Grants EAR-87-08276 and EAR-82-12764 for purchase of the STEM and EMPA, respectively.

References

Aguirre L, Atherton MP (1987) Low-grade metamorphism and geotectonic setting of Macuchi Formation, west Cordillera of Equator. J Metam Geol 5:473–494

Ahn JH, Peacor DR (1985) Transmission electron microscopic study of diagenetic chlorite in Gulf Coast argillaceous sediments. Clays Clay Miner 33:228–236

Ahn JH, Peacor DR (1986) Transmission electron microscope data for rectorite: implications for the origin and structure of "fundamental particles". Clays Clay Miner 34:180–186

Ahn JH, Peacor DR, Coombs DS (1988) Formation mechanisms of illite, chlorite and mixed-layer illite-chlorite in Triassic volcanogenic sediments from the Southland Syncline, New Zealand. Contrib Mineral Petrol 99:82–89

Albee AL (1962) Relationships between the mineral association, chemical composition and physical properties of the chlorite series. Am Mineral 47:851–870

Alietti A (1958) Some interstratified clay minerals of the Taro Valley. Clay Miner Bull 3:207–211

Almon WR, Fullerton LB, Davies DK (1976) Pore space reduction in Cretaceous sandstones through chemical precipitation of clay minerals. J Sediment Petrol 46:89–96

Alt JC, Laverne C, Muehlenbachs K (1985) Alteration of the upper oceanic crust: mineralogy and process in DSDP Hole 504B, Leg 83. Initial Rep DSDP 83:217–241

April RH (1981) Trioctahedral smectite and interstratified chlorite/smectite in Jurassic strata of the Connecticut Valley. Clays Clay Miner 29:31–39

Bailey SW (1980) Structures of layer silicates. In: Brindley GW, Brown G (eds) Crystal structures of clay minerals and their X-ray identification. Mineralogical Society, London, pp 1–123

Bailey SW (1981) Nomenclature for regular interstratifications. Clay Sci 5:305–311

Bailey SW (1988) Chlorites: structures and crystal chemistry. In: Bailey SW (ed) Hydrous phyllosilicates (Reviews in mineralogy, vol 19). Mineralogical Society of America, Washington DC, pp 347–403

Baltatzis EG, Katagas CG (1984) The pumpellyite-actinolite and contiguous facies in part of Phyllite-Quartzite Series, central Northern Peloponnesus, Greece. J Metam Geol 2:349–363

Bettison LA, Schiffman P (1988) Compositional and structural variations of phyllosilicates from the Point Sal ophiolite, California. Am Mineral 73:62–76

Bettison-Varga LA, Mackinnon IDR (1989) Comparison of microanalytical techniques used in the characterization of mixed-layer chlorite/smectite from Point Sal Ophiolite (abstract). Clay Minerals Society, 26th Annual Meeting

Black PM (1975) Mineralogy of New Caledonia metamorphic rocks, IV. Sheet silicates from the Quegoa district. Contrib Mineral Petrol 49:269–284

Blatter CL, Roberson HE, Thompson GR (1973) Regularly interstratified chlorite-dioctahedral smectite in dike-intruded shale, Montana. Clays Clay Miner 21:207–212

Bloss DF (1971) Crystallography and crystal chemistry. Holt, Rinehart and Winston, New York

Boles JR, Coombs DS (1975) Mineral reactions in zeolitic Triassic tuff, Hokonui Hills, New Zealand. Geol Soc Am Bull 86:163–173

Boles JR, Coombs DS (1977) Zeolite facies alteration of sandstones in the Southland Syncline, New Zealand. Am J Sci 277:982–1012

Bradley WF, Weaver CE (1956) A regularly interstratified chlorite-vermiculite clay minerals. Am Mineral 41:497–504

Brigatti MF, Poppi L (1984a) "Corrensite-like minerals" in the Taro and Ceno Valleys, Italy. Clay Miner 19:59–66

Brigatti MF, Poppi L (1984b) Crystal chemistry of corrensite: a review. Clays Clay Miner 32:391–399

Cathelineau M, Izquierdo G (1988) Temperature-composition relationships of authigenic micaceous minerals in the Los Azufres geothermal system. Contrib Mineral Petrol 100:418–428

Cathelineau M, Nieva D (1985) A chlorite solid solution geothermometer. The Los Azufres (Mexico) geothermal system. Contrib Mineral Petrol 91:235–244

Champness PE, Cliff G, Lorimer GW (1981) Quantitative analytical electron microscopy. Bull Mineral 104:236–240

Chang HK, Mackenzie FT, Schoonmaker J (1986) Comparisons between the diagenesis of dioctahedral and trioctahedral smectite, Brazilian offshore basins. Clays Clay Miner 34:407–423

Chen CH, Chu HT, Liou JG, Ernst WG (1983) Explanatory notes for the metamorphic facies map of Taiwan. Cent Geol Surv ROC Spec Pub 2

Cho M, Liou JG, Maruyama S (1986) Transition from the zeolite to prehnite-pumpellyite facies in Karmutsen metabasites. Vancouver Island, British Columbia. J Petrol 27:467–494

Cliff G, Lorimer GW (1975) The quantitative analysis of thin specimens. J Microsc 103:203–207

Cooper AF (1972) Progressive metamorphism of metabasic rocks from the Haast schist group of southern New Zealand. J Petrol 13:457–492

Craw D, Jamieson RA (1984) Anomalous optics in low-grade chlorite from Atlantic Canada. Can Mineral 22:269–280

Curtis CD, Hughes CR, Whiteman JA, Whittle CK (1985) Compositional variation within some sedimentary chlorites and some comments on their origin. Mineral Mag 49:375–386

Dallmeyer RD (1974) The role of crystal structure in controlling the partitioning of Mg and Fe^{2+} between coexisting garnet and biotite. Am Mineral 59:201–203

Earley JW, Brindley GW, McVeagh WJ, Vanden Heuvel RC (1956) A regularly interstratified montmorillonite-chlorite. Am Mineral 41:258–267

Eggleton RA, Banfield JF (1985) The alteration of granitic biotite to chlorite. Am Mineral 70:902–910

Ernst WG, Seki Y, Onuki H, Gilbert MC (1970) Comparative study of low-grade metamorphism in the California coast range and the outer metamorphic belt of Japan. Geol Soc Am Mem 124:1–259

Evarts RC, Schiffman P (1983) Submarine hydrothermal metamorphism of the Del Puerto ophiolite, California. Am J Sci 283:289–340

Ferry JM, Mutti LJ, Zuccala GJ (1987) Contact metamorphism/hydrothermal alteration of Tertiary basalts from the Isle of Skye, northwest Scotland. Contrib Mineral Petrol 95:166–181

Foster MD (1962) Interpretation of the composition and classification of the chlorites. US Geol Surv Prof Pap 414-A:1–33

Franceschelli M, Mellini M, Memmi I, Ricci CA (1986) Fine-scale chlorite-muscovite association in low-grade metapelites from Nurra (NW Sardinia), and the possible misidentification of metamorphic vermiculite. Contrib Mineral Petrol 93:137–143

Furbish WJ (1975) Corrensite of deuteric origin. Am Mineral 60:928–930

Güven N (1988) Smectites. In: Bailey SW (ed) Hydrous phyllosilicates (Reviews in mineralogy, vol 19). Mineralogical Society of America, Washington DC, pp 497–559

Iijima A, Utada M (1971) Present-day diagenesis of the Neogene geosynclinal deposits in the Niigata oilfield, Japan. In: Gould RF (ed) Molecular sieve zeolites-I (Advances in chemistry, Series 101). American Chemical Society, Washington DC, pp 342–349

Iijima S, Zhu J (1982) Electron microscopy of a muscovite-biotite interface. Am Mineral 67:1195–1205

Inoue A, Utada M, Negata H, Watanabe T (1984) Conversion of trioctahedral smectite to interstratified chlorite/smectite in Pliocene acidic pyroclastic sediments of the Ohyu district, Akita Prefecture, Japan. Clay Sci Soc Japan 6:103–116

Johnson LJ (1964) Occurrence of regularly interstratified chlorite-vermiculite as a weathering product of chlorite in a soil. Am Mineral 49:556–572

Kawachi Y (1975) Pumpellyite-actinolite and contiguous facies metamorphism in part of Upper Wakatipu district, South Island, New Zealand. NZJ Geol Geophy 18:401–441

Klimentidis RE, Mackinnon DR (1986) High-resolution imaging of ordered mixed-layer clays. Clays Clay Miner 34:155–164

Kopp OC, Fallis SM (1974) Corrensite in the Willington Formation, Lyons, Kansas. Am Mineral 59:623–624

Kranidiotis P, MacLean WH (1987) Systematics of chlorite alteration at the Phelps Dodge massive sulfide deposit, Matagami, Quebec. Econ Geol 82:1898–1911

Kristmannsdóttir H (1975) Clay minerals formed by hydrothermal alteration of basaltic rocks in Icelandic geothermal fields. Geol Foren Stockholm Forhand 97:289–292

Kristmannsdóttir H (1979) Alteration of basaltic rocks by hydrothermal activity at 100–300° C. In: Mortland MM, Farmer VC (eds) International Clay Conference 1978. Elsevier, Amsterdam, pp 359–367

Laird J (1988) Chlorites: metamorphic petrology. In: Bailey SW (ed) Hydrous phyllosilicates (Reviews in mineralogy, vol 19). Mineralogical Society of America, Washington DC, pp 405–453

Lee JH, Peacor DR, Lewis DD, Wintsch RP (1984) Chlorite-illite/muscovite interlayered and interstratified crystals: a TEM/STEM study. Contrib Mineral Petrol 88:372–385

Leitch EC (1975) Zonation of low grade regional metamorphic rocks, Nambucca Slate Belt, northeastern South Wales. J Geol Soc Aust 22:413–422

Lippmann F (1954) Über einen Keuperton von Kaiserweiher bei Maulbronn. Heidelb Beitr Mineral Petrogr 4:130–144

Lippmann F (1956) Clay minerals from the Röt member of the Triassic near Göttingen, Germany. J Sediment Petrol 26:125–139

Lippmann F (1979) Stability diagrams involving clay minerals. 8th Conference of Clay Mineralogy and Petrology, Teplice

Lippmann F (1981) The thermodynamic status of clay minerals. In: Van Olphen H, Veniale F (eds) International Clay Conference 1981. Elsevier, Amsterdam, pp 475–485

Newman ACD, Brown G (1987) The chemical constitution of clays. In: Newman ACD (ed) Chemistry of clays and clay minerals. Wiley, New York, pp 1–128

Nutt CJ (1989) Chloritization and associated alteration at the Jabiluka unconformity-type uranium deposit, Northern Territory, Australia. Can Mineral 27:41–58

Olives J (1985) Biotites and chlorites as interlayered biotite-chlorite crystals. Bull Mineral 108:635–641

Olives J, Amouric M (1984) Biotite chloritization by interlayer brucitization as seen by HRTEM. Am Mineral 69:869–871

Olives J, Amouric M, De Fouquet C, Baronnet A (1983) Interlayering and slip in biotite as seen by HRTEM. Am Mineral 68:754–758

Pollastro RM (1988) Clay mineralogy and diagenetic evolution of deeply buried rocks of the Simpson Group (middle Ordovician), Anadarko Basin, Oklahoma (abstract). Clay Minerals Society, 25th Annual Meeting

Reynolds RC Jr (1980) Interstratified clay minerals. In: Brindley GW, Brown G (eds) Crystal structures of clay minerals and their X-ray identification. Mineralogical Society, London, pp 249–303

Reynolds RC Jr (1985) NEWMOD, a computer program for the calculation of one-dimensional diffraction patterns of mixed-layered clays. Reynolds RC, 8 Brook Rd, Hanover, New Hampshire 03755, USA

Reynolds RC Jr (1988) Mixed layer chlorite minerals. In: Bailey SW (ed) Hydrous phyllosilicates (Reviews in mineralogy, vol 19). Mineralogical Society of America, Washington DC, pp 601–629

Roberson HE (1987) Corrensite and chlorite in subseafloor hydrothermal altered basalts (abstract). Clay Minerals Society, 24th Annual Meeting

Roberson HE (1988) Random mixed-layer chlorite-smectite: does it exist? (abstract) Clay Minerals Society, 25th Annual Meeting

Schreyer W, Medenbach O, Abraham K, Gebert W, Muller WF (1982) Kulkeite, a new metamorphic phyllosilicate mineral: ordered 1:1 chlorite/talc mixed-layer. Contrib Mineral Petrol 80:103–109

Shau Y-H, Peacor DR, Essene EJ (1988) A TEM/AEM study of chloritic minerals and corrensite in metabasalt from northern Taiwan (abstract). Clay Minerals Society, 25th Annual Meeting

Shau Y-H, Peacor DR (1988) A TEM study of trioctahedral phyllosilicates as alteration products of olivine in basalts of DSDP Hole 504B (abstract). Geological Society of America, Abstracts with Program, 20

Shau Y-H, Peacor DR (1989) Phyllosilicates in hydrothermally altered basalts from DSDP Hole 504B, Leg 83 – a TEM/AEM study (abstract). Geological Society of America, Abstracts with Program, 21

Shau Y-H, Yang H-Y (1987) Petrology of basaltic rocks from Junghua, Taoyuanhsien, northern Taiwan. Proc Geol Soc China 30:58–82

Shikazono N, Kawahata H (1987) Compositional differences in chlorite from hydrothermally altered rocks and hydrothermal ore deposits. Can Mineral 25:465–474

Shirozu H (1978) Chlorite minerals. In: Sudo T, Shimoda S (eds) Clays and clay minerals of Japan. Elsevier, Amsterdam, pp 243–264

Shirozu H, Sakasegawa T, Katsumoto N, Ozaki M (1975) Mg-chlorite and interstratified Mg-chlorite/saponite associated with Kuroko deposits. Clay Sci 4:305–321

Smith WW (1960) Some interstratified clay minerals from basic igneous rocks. Clay Miner Bull 4:182–190

Steinfink H (1958) The crystal structure of chlorite. I. A monoclinic polymorph. Acta Cryst 11:191–195

Strens RGJ, Freer R, Firman RJ (1987) Stability of chlorite-quartz assemblages in rocks south and west of Keswick, Cumbria. Mineral Mag 51:649–654

Vali H, Koster HM (1986) Expanding behaviour, structural disorder, regular and random irregular interstratification of 2:1 layer-silicates studied by high-resolution images of transmission electron microscopy. Clay Miner 21:827–859

Veblen DR (1983) Microstructures and mixed layering in intergrown wonesite, chlorite, talc, biotite and kaolinite. Am Mineral 68:566–580

Veblen DR, Ferry JM (1983) A TEM study of biotite-chlorite reaction and composition with petrologic observations. Am Mineral 68:1160–1168

Velde B (1977) A proposed phase diagram for illite, expanding chlorite, corrensite and illite-montmorillonite mixed layered minerals. Clays Clay Miner 25:264–270

Viereck LG, Griffin BJ, Schmincke H-U, Pritchard RG (1982) Volcaniclastic rocks of the Reydarfjordur Drill Hole, eastern Iceland, 2. alteration. J Geophys Res 87:6459–6476

Walshe JL (1986) A six-component chlorite solid solution model and the conditions of chlorite formation in hydrothermal and geothermal systems. Econ Geol 81:681–703

White SH, Huggett JM, Shaw HF (1985) Electron-optical studies of phyllosilicate intergrowths in sedimentary and metamorphic rocks. Mineral Mag 49:413–423

Yang H-Y, Shau Y-H (1988) Occurrence of pumpellyite-bearing basaltic tuffs in Hsuehshan Range. Proc Geol Soc China 31:24–32

Yau Y-C, Anovitz LM, Essene EJ, Peacor DR (1984) Phlogopite-chlorite reaction mechanisms and physical conditions during retrograde reactions in the Marble Formation, Franklin, New Jersey. Contrib Mineral Petrol 88:299–306

Editorial responsibility: J.M. Ferry